

Modelled density surfaces of cetaceans in European Atlantic waters in summer 2016 from the SCANS-III aerial and shipboard surveys

C. Lacey¹, A. Gilles², P. Börjesson³, H. Herr⁴, K. Macleod⁵, V. Ridoux⁶, M.B. Santos⁷, M. Scheidat⁸, J. Teilmann⁹, S. Sveegaard⁹, J. Vingada¹⁰, S. Viquerat⁴, N. Øien¹¹ & P.S. Hammond¹

1. University of St Andrews, UK
2. University of Veterinary Medicine, Hannover, Germany
3. Swedish University of Agricultural Sciences, Sweden
4. University of Hamburg, Germany
5. Joint Nature Conservation Committee, UK
6. University of La Rochelle, France
7. Instituto Español de Oceanografía, Centro Oceanográfico de Vigo, Spain
8. Wageningen Marine Research, Netherlands
9. Aarhus University, Denmark
10. Sociedade Portuguesa de Vida Selvagem, Portugal
11. Institute of Marine Research, Norway

SCANS-III project report 2, 31pp + Appendices.

INTRODUCTION

A series of large-scale surveys for cetaceans in European Atlantic waters was initiated in 1994 in the North Sea and adjacent waters (SCANS 1995; Hammond et al., 2002) and continued in 2005 in all shelf waters (SCANS-II 2008; Hammond et al., 2013) and 2007 in offshore waters (CODA 2009). In the mid-1990s, the primary need for a large-scale survey was to obtain the first comprehensive estimates of abundance of harbour porpoise in the North Sea and adjacent waters so that estimates of bycatch could be placed in a population context. The motivation for ongoing surveys is to provide information at an appropriately wide spatial scale on distribution and abundance of cetaceans to facilitate reporting by Member States on Favourable Conservation Status under the Habitats Directive and, particularly, on Good Environmental Status (GES) under the Marine Strategy Framework Directive (MSFD).

The frequency of these surveys was intended to be approximately decadal, and a new survey was thus scheduled for the mid-2010s. The previous SCANS projects had been supported by the European LIFE Nature programme but a proposal for a SCANS-III project with a survey to take place in 2015 was rejected without review. Member States nevertheless remained committed to the project and sufficient resources were secured to conduct the SCANS-III survey in summer 2016. The supporting countries were Denmark,

France, Germany, the Netherlands, Norway, Portugal, Spain, Sweden and the UK. The independent project ObSERVE conducted surveys in Irish waters during the period 2015-2017 (Rogan et al., 2018).

A primary aim of SCANS-III was to provide robust large-scale estimates of cetacean abundance to inform the upcoming MSFD assessment of GES in European Atlantic waters in 2018. Design-based estimates of abundance are presented in Hammond et al. (2021). An additional aim of SCANS-III was to provide information on summer distribution by modelling the data in relation to spatially linked environmental features to generate density surface maps.

This report describes the density surface modelling for those cetacean species for which sufficient data were obtained during SCANS-III: harbour porpoise (*Phocoena phocoena*), bottlenose dolphin (*Tursiops truncatus*), white-beaked dolphin (*Lagenorhynchus albirostris*), common dolphin (*Delphinus delphis*), striped dolphin (*Stenella coeruleoalba*), long-finned pilot whale (*Globicephala melas*), all beaked whale species combined (Ziphiidae), minke whale (*Balaenoptera acutorostrata*) and fin whale (*Balaenoptera physalus*).

To compare the results for 2016 with those from 2005/07, data from the SCANS-II (2005) and CODA (2007) surveys were also reanalysed.

DATA SOURCES AND PROCESSING

The SCANS-III study area and survey design are described in Hammond et al. (2021). The area surveyed, and areas of other surveys conducted at around the same time are shown in Figure 1. Ship and aerial survey data collection methods are also described in Hammond et al. (2021).

The SCANS-II and CODA study areas, survey design and data collection methods are described in Hammond et al. (2013) and CODA (2009). The survey area and blocks are shown in Figure 2.

For SCANS-III in 2016, the cetacean data used in the analysis were the same as those used to obtain design-based estimates of abundance presented in Hammond et al. (2021). For SCANS-II and CODA in 2005/07, the cetacean data were those previously analysed in Hammond et al. (2013), CODA (2009) and Rogan et al. (2017).

Spatially referenced data on features of the environment used as covariates in the analysis are described in Table 1. Geographic Cartesian coordinates (easting, X, and northing, Y) were included because the aim of the analysis was to find the best prediction of cetacean distribution represented by the available data, and Cartesian coordinates typically account for much of the variability in the data in density surface models. The environmental covariates were selected from available data because they were believed to have the potential to explain additional variability in cetacean density. Data for other potentially useful covariates (e.g., currents, fronts) were not available over the whole range of the study area. The inclusion of Cartesian coordinates can impact the modelled relationships between density and environmental covariates so caution is needed when drawing inference from the results about how these environmental covariates may explain distribution.

The spatial resolution of the fitted models was approximately 10km and the spatial resolution of the model predictions was 10x10km (see (d) and (g) below).

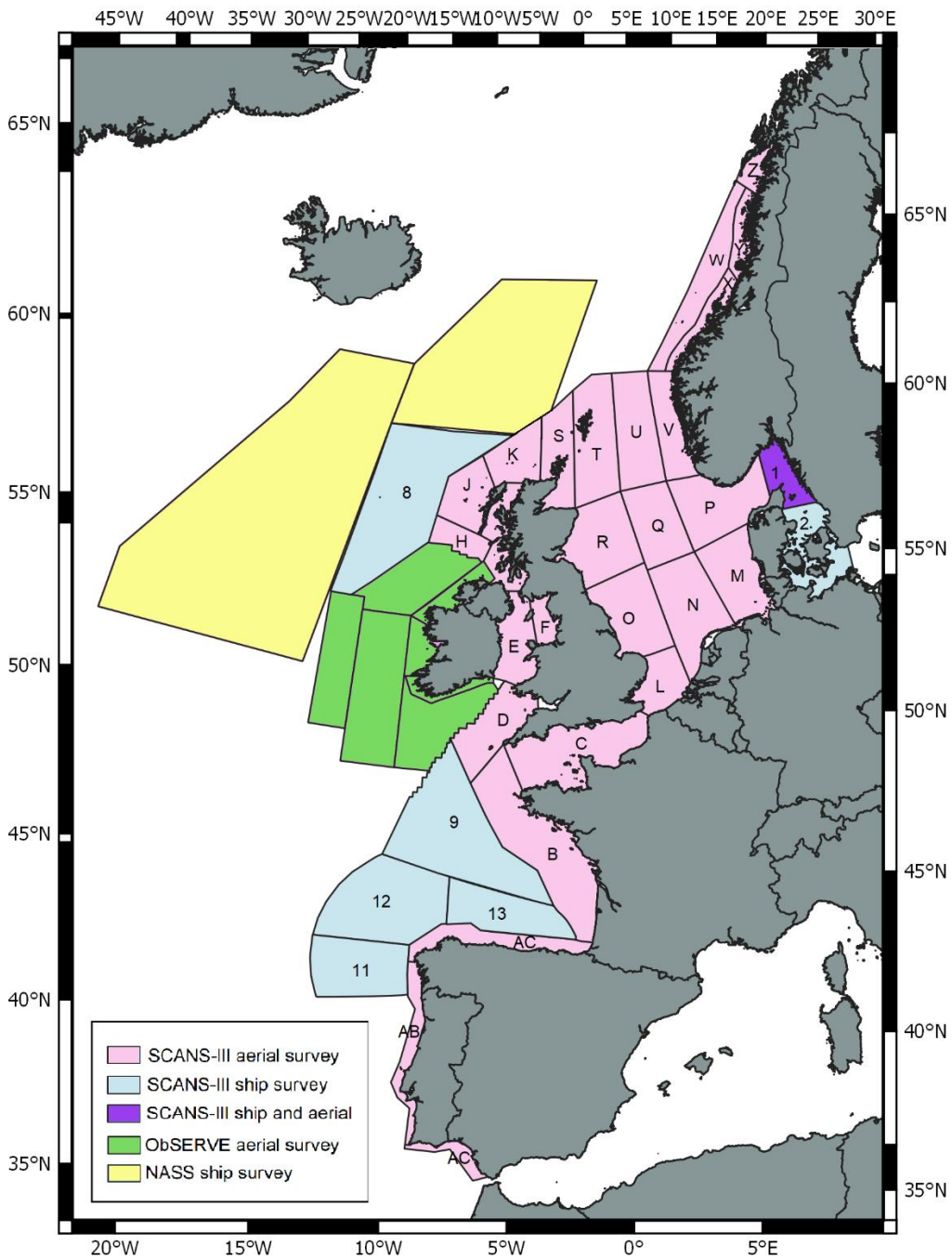


Figure 1. Area covered by SCANS-III and adjacent surveys. SCANS-III: pink lettered blocks were surveyed by aircraft; pale blue numbered blocks were surveyed by ship. Block 1 (purple) was also surveyed by aircraft because the weather was poor during the ship survey in this block. Blocks coloured green to the south, west and north of Ireland were surveyed by the Irish ObSERVE project in 2015-2017. Blocks coloured yellow were surveyed by the Faroe Islands as part of the North Atlantic Sightings Survey (NASS) in 2015 (Pike et al., 2019).

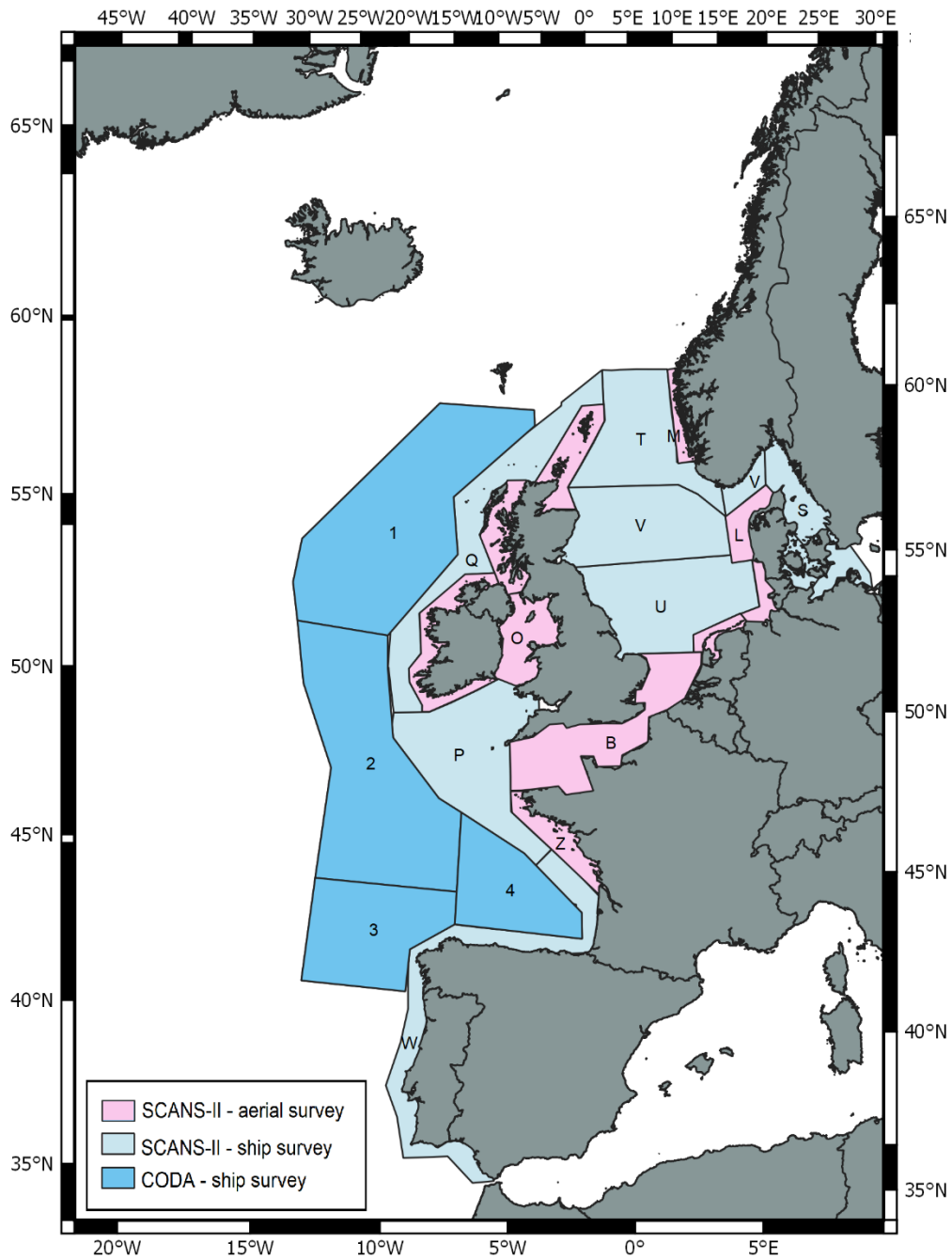


Figure 2. Area covered by SCANS-II and CODA surveys. SCANS-II blocks (letters) were surveyed in 2005: pink blocks were surveyed by aircraft; pale blue blocks were surveyed by ship. CODA blocks (numbers) were surveyed in 2007 by ship.

Table 1: Covariates used in the density surface modelling. Data from NEODAAS, the NERC Earth Observation Data Acquisition and Analysis Service (<https://www.neodaas.ac.uk/>), were available at a spatial resolution of 9km. ETOPO1 data are from a 1 arc-minute global relief model (<https://ngdc.noaa.gov/mgg/global/global.html>).

Covariate	Description	Data source
X	Longitude converted to UTM30: 32360 coordinates	
Y	Latitude converted to UTM30: 32360 coordinates	
Depth of seabed (Depth)	Mean depth (m) calculated over a buffer of 5km radius using R package marmap	ETOPO1 database, hosted by NOAA (Amante & Eakins, 2009). Pante & Simon-Bouhet (2013)
Standard deviation of Depth (Depth SD)	Standard deviation of depth (m) calculated over a buffer of 5km radius using R package marmap. Acts as an indicator of variability in the seabed	ETOPO1 database, hosted by NOAA (Amante & Eakins, 2009). Pante & Simon-Bouhet (2013)
Slope	Slope of the seabed (°) extracted from single point location using R package marmap	ETOPO1 database, hosted by NOAA (Amante & Eakins, 2009). Pante & Simon-Bouhet (2013)
Aspect	The direction that the slope faces (°). Extracted from single point location using R package marmap	ETOPO1 database, hosted by NOAA (Amante & Eakins, 2009). Pante & Simon-Bouhet (2013)
Absolute distance from coast (Dist coast)	Distance at shortest point (km)	ETOPO1 database, hosted by NOAA (Amante & Eakins, 2009)
Absolute distance from 50m isobath (Dist 50)	Distance at shortest point (km)	ETOPO1 database, hosted by NOAA (Amante & Eakins, 2009)
Absolute distance from 200m isobath (Dist 200)	Distance at shortest point (km)	ETOPO1 database, hosted by NOAA (Amante & Eakins, 2009)
Absolute distance from 2000m isobath (Dist 2000)	Distance at shortest point (km)	ETOPO1 database, hosted by NOAA (Amante & Eakins, 2009)
Distance from 50m isobath (CS 50)	Distance at shortest point (km); negative on deeper side	ETOPO1 database, hosted by NOAA (Amante & Eakins, 2009)
Distance from 200m isobath (CS 200)	Distance at shortest point (km); negative on deeper side	ETOPO1 database, hosted by NOAA (Amante & Eakins, 2009)
Absolute Dynamic Topography (ADT)	Departure of sea surface level from the geoid due to ocean dynamics (m). Calculated from the sea level anomaly (SLA) and the mean dynamic topography (MDT): $ADT = SLA + MDT$	Data produced by the Copernicus Marine Environment Monitoring Service (CMEMS) Sea Level-TAC multimission altimetry processing system, and processed and provided by NEODAAS
Sea Level Anomaly (SLA)	Difference between sea surface height and mean sea surface (m). Sea surface height derived from satellite altimetry, and mean sea surface calculated from 20 years of these data.	Data produced by the Copernicus Marine Environment Monitoring Service (CMEMS) Sea Level-TAC multimission altimetry processing system, and processed and provided by NEODAAS
Sea Surface Temperature (SST)	Optimally Interpolated (OI) merged microwave-infrared SST (°C) product from Remote Sensing Systems.	Data provided by NEODAAS

Data from the aerial and ship surveys were processed in the same way. Segments of searching effort were created from the raw data in a series of steps.

- (a) Short sections of searching effort, with associated sightings, were created and spatially referenced by linking the effort data files to the geographical positions recorded every 4 seconds on the aerial surveys and every 10 seconds on the ship surveys. Given survey speeds of approximately $185 \text{ km}\cdot\text{h}^{-1}$ (aerial) and $18.5 \text{ km}\cdot\text{h}^{-1}$ (ship), these sections were approximately 200m in length for the aerial survey and approximately 50m for the ship survey. On the few occasions when the GPS signal was missing for a short period in the ship data, positions were interpolated linearly. For the ship surveys, only data collected from the primary platform in 0-4 Beaufort (0-2 Beaufort for harbour porpoise) were used. For the aerial surveys, data collected under moderate and good “subjective” sighting conditions (defined in reference to harbour porpoises, the most challenging species to detect) were used, excluding repeat effort and sightings from the circle-back procedure (see Hammond et al., 2021).
- (b) Sighting-condition-specific estimates of the total effective strip width (esw, including both sides of the transect line) were linked to these short sections of effort based on the sighting conditions prevailing during that period of searching. For aerial surveys, sighting conditions were defined using the “subjective” measure (see above). For shipboard surveys, sighting conditions were defined using the Beaufort scale, swell strength and a general measure of sightability (defined in reference to dolphins). For SCANS-III, these estimates of esw were derived from the detection functions fitted for each species (Hammond et al., 2021). For SCANS-II and CODA, they were derived from previous analyses of these data (Hammond et al., 2013; CODA, 2009; Rogan et al., 2017). For most species, these estimates of esw incorporated corrections for animals missed on the transect line, through the aerial survey circle-back procedure (harbour porpoise, all dolphin species, minke whale) and the ship survey double team mark-recapture distance analysis (all species except sperm whale, beaked whale in 2005/07, and minke whale in 2016) (see Hammond et al., 2021). The effective area searched in each short section of effort was calculated as the esw multiplied by the distance travelled.
- (c) Values of depth, slope and aspect were linked to these short sections of effort.
- (d) Segments of effort of target 10km length were created by joining consecutive short sections of effort using function `segmentate` in R (Viquerat, pers. comm; R Core Team 2020). Values of effective area searched were summed over all short sections of effort for each segment. Segments less than 1 km in length at the ends of survey tracks were excluded.
- (e) Mean depth, slope and aspect, averaged over short effort sections, were linked to each segment. Values of distance from the coast and from the 50m, 200m and 2000m isobaths were calculated for the midpoint of each segment. These effort segments formed the sampling unit for data analysis.
- (f) Data for dynamic covariates were provided by NEODASS (<https://www.neodaas.ac.uk/>) as netCDF files. These were converted to raster files, and a weighted mean value across a 10km diameter circle centred at the mid-point of the segment was calculated and linked to the segment.
- (g) A 10x10km spatial grid was created and values of the environmental variables were associated with each grid cell in the same way as described above for the effort segments. The grid was used as a basis for predicting cetacean density spatially from the fitted models using the values of the environmental variables in each grid cell.

All data processing was undertaken in software R version 4.0.3 (R Core Team 2020).

DATA ANALYSIS

Model structure, fitting and selection

Modelling methods using Generalised Additive Models (GAM) followed the framework outlined in Gilles et al. (2016), Becker et al. (2016; 2017) and Rogan et al. (2017). The general structure of the model, using a logarithmic link function, was:

$$n_i = \exp \left[\ln(a_i) + \theta_0 + \sum f_k(z_{ik}) \right]$$

where the response variable n_i is the number of individuals detected in the i^{th} effort segment, the offset a_i is the effective area searched for the i^{th} segment, θ_0 is the intercept, f_k are smoothed functions of the explanatory environmental covariates, and z_{ik} is the value of the k^{th} explanatory covariate in the i^{th} segment. Tweedie and negative binomial distributions were considered as candidate error distributions for the response variable to account for over-dispersion in the count data, with the over-dispersion parameter estimated during model fitting.

Smooth functions were fitted using restricted maximum likelihood (REML) with automatic term selection (Marra & Wood, 2011). Thin-plate regression splines were used for all covariates except for Aspect for which a cyclic penalized cubic regression spline was used. Covariates X and Y were included in all models as a 2-dimensional isotropic smooth. The maximum number of knots allowed in fitting was set at 10 for single covariates and 30 for the isotropic smooth, but these maxima were never approached in any model (see Results).

This model-fitting method helps to avoid overfitting of the smooth functions by including a modification to penalize slightly the null space (Marra & Wood, 2011). The method can reduce the estimated degrees of freedom of a covariate term towards zero if it does not contribute sufficiently to explaining the variability in the data. For each species, following initial fitting of a model including all candidate uncorrelated covariates, those covariates with estimated degrees of freedom of 0.5 or less were removed from the model. Model goodness of fit was assessed by inspection of QQ plots and plots of model residuals.

To avoid including correlated covariates in the models, correlation matrices were calculated for the SCANS-III data and for SCANS-II/CODA data to identify which explanatory variables were correlated. Where variables were correlated (Appendix A.1), a set of models for each species was first run with each variable as a single covariate and the model with the lowest Akaike's Information Criterion (AIC) determined which covariate to include in subsequent modelling. This primarily happened with distance to coast, 50m, 200m, 2000m isobath covariates, with SST and ADT, and with Standard Deviation of Depth and Slope.

For two species (common dolphin and striped dolphin), models of individual numbers did not fit the data well because the greater range of group sizes recorded for these species caused severe over-dispersion in the distribution of counts of individuals. For these species, the number of groups in each effort segment was modelled as the response variable, rather than number of individuals. Estimated densities of groups predicted from the selected models (see Results) were then multiplied by observed mean group size to generate estimates of individual density, equivalent to estimates from models of individuals for the other

species. Models of common dolphin and striped dolphin group size were fitted but none resulted in an improvement on mean group size so predictions from these models were not used.

Model application

Models were fitted to all data in SCANS-III in 2016 and all data in SCANS-II/CODA in 2005/2007 for bottlenose dolphin, white-beaked dolphin, common dolphin, striped dolphin, pilot whale, all beaked whale species combined, minke whale and fin whale.

For harbour porpoise modelling, data were restricted to survey blocks in shelf waters. Sightings of this species in deeper waters off the shelf are very rare in the European Atlantic (Reid et al., 2003). In SCANS-III in 2016, no harbour porpoises were seen in blocks 8, 9, 11, 12 and 13 (Figure 1), except for a small number of animals close to Rockall in the west of block 8 (Hammond et al., 2021). Block 8 was nevertheless excluded from the modelling because including it would likely have adversely influenced the modelled relationships for the rest of the survey area and led to a false impression of distribution in the waters between Rockall and Scotland/Ireland. No harbour porpoises were seen in CODA in 2007 so only data from SCANS-II in 2005 were modelled.

For SCANS-III in 2016, a single model fitted to all harbour porpoise data generated a strong “edge-effect” (lack of fit at the edge of covariate space) which led to a poor prediction of distribution in block 2. Attempts to resolve this lack of fit using methods that account for land boundaries or allow spatial smoothing at different scales in different areas (e.g., SOAP or CReSS; Wood et al. 2008; Scott-Hayward et al. 2014) were unsuccessful. Consequently, the harbour porpoise data for SCANS-III block 2 were modelled separately. In contrast, no problems were encountered fitting a single harbour porpoise model to all SCANS-II data in 2005, or for any other species.

For each species, density from the selected best model was predicted onto the 10x10km spatial grid.

The coefficient of variation (CV) of predicted density in each grid cell was estimated based on posterior simulation of the model results. 1,000 vectors of the model coefficients were simulated using function `mvrnorm` from the MASS library in R (Venables & Ripley, 2002), from which 1,000 predictions of density in each grid cell were made. The standard error and hence CV of density was calculated from the 1,000 predictions.

Harbour porpoise distribution was predicted only in shelf waters, reflecting the data used in analysis. For 2016, harbour porpoise predictions from the model for block 2 and the model for all other blocks in shelf waters were joined. For other species, predictions in 2016 excluded block 2.

All modelling was conducted using package `mgcv` (Wood, 2017) in software R version 4.0.3 (R Core Team 2020). Density surfaces were plotted on maps using software QGIS v3.4 Madeira (QGIS, 2021).

RESULTS

Searching effort and sightings

Tables 2 and 3 summarise the effort and sightings data for each species used in analysis of the SCANS-III data in 2016 and SCANS-II/CODA data in 2005/2007, respectively. Except for harbour porpoise, the percentage of segments with sightings of groups was small: around 3-6% for common dolphin, common and striped dolphins, and fin whale, and around 1% or fewer for the other species, illustrating the extent of over-dispersion in the data.

Table 2. Number of effort segments and number of groups and individuals sighted of each species used in analysis of the SCANS-III data in 2016. Effort in 0-2 Beaufort only for harbour porpoise, and 0-4 Beaufort for all other species.

Species	Total no. of effort segments	No. of effort segments with groups	% effort segments with groups	Number of groups	Number of individuals
Harbour porpoise (excluding block 2)	4,532	857	18.9	1,475	1,994
Harbour porpoise (block 2 only)	98	65	66.3	285	377
Bottlenose dolphin	5,293	58	1.1	71	325
White-beaked dolphin	5,293	64	1.2	107	419
Common dolphin	5,293	217	4.1	539	4,701
Striped dolphin	5,293	53	1.0	74	1,974
Common, striped and unid. common or striped dolphins	5,923	369	6.2	904	8,711
Pilot whale	5,293	38	0.7	55	264
Beaked whales	5,293	39	0.7	41	68
Fin whale	5,293	259	4.9	565	796
Minke whale	5,293	68	1.3	77	81

Table 3. Number of effort segments and number of groups and individuals sighted of each species used in analysis of the SCANS-II and CODA data in 2005/07. Effort in 0-2 Beaufort only for harbour porpoise, and 0-4 Beaufort for all other species.

Species	Total no. of effort segments	No. of effort segments with groups	% effort segments with groups	Number of groups	Number of Individuals
Harbour porpoise	2,292	449	19.6	874	1,355
Bottlenose dolphin	4,051	44	1.1	49	404
White-beaked dolphin	4,051	32	0.8	37	183
Common dolphin	4,051	146	3.6	265	3,713
Striped dolphin	4,051	26	0.6	32	532
Common, striped and unid. common or striped dolphins	4,051	189	4.7	347	5,063
Pilot whale	4,051	30	0.7	47	300
Beaked whales	4,051	24	0.6	25	59
Fin whale	4,051	129	3.2	190	291
Minke whale	4,051	64	1.6	82	87

Model results and predicted density surfaces

Summary results of the final selected models fitted to data from SCANS-III (2016) and from SCANS-II and CODA (2005/07) for each species are given in Tables 4-13. Model diagnostics and plots of the fitted smooth functions are given in Appendix A.2 for SCANS-III and A.3 for SCANS-II/CODA. The error distribution was best described by the negative binomial distribution in 13 models and by the Tweedie distribution in six models. All models, except one (beaked whales in 2016, Table 11), retained the 2-dimensional isotropic smooth function of geographical coordinates, $s(X, Y)$, and all models included one or more additional covariates.

The estimated degrees of freedom (edf) associated with the fitted smooth functions were generally much greater for $s(X, Y)$ than for other covariates. For some additional covariates, the edf was less than 1, indicative of a linear relationship with wide confidence intervals (see Appendices A.2 and A.3). These covariates thus contribute little to model fit but were nevertheless retained during model fitting.

The final models explained more than 50% of the deviance for the majority of species, indicating that the models fitted the data fairly well (Tables 4-13). The species with the lowest values of explained deviance were harbour porpoise (27% and 23% in 2016 [excluding block 2] and 2005/07, respectively), minke whale (24% and 39%), bottlenose dolphin (38% and 28%), and striped dolphin (40% and 48%).

Most of the variability in the data was accounted for by the 2-dimensional smooth functions of Cartesian coordinates, which were included to obtain the best prediction of distribution from the data. The importance of the other environmental covariates retained in each model or the nature of the fitted relationships are not discussed.

Table 4. Model description and diagnostics for the final selected models of **harbour porpoise** individuals in SCANS-III (2016) and SCANS-II (2005). Covariates in the models are described in Table 1.

Dataset	Error distribution	Model covariates	Estimated degrees of freedom	Model degrees of freedom	% Deviance explained
SCANS-III (2016) excluding block 2	Negative binomial	X, Y	20.1	26.3	27
		Depth	0.9		
		ADT	3.3		
		CS 200	1.0		
SCANS-III (2016) block 2 only	Tweedie	X, Y	10.7	14.7	49
		Depth	2.4		
		Dist coast	0.6		
SCANS-II (2005)	Negative binomial	X, Y	22.8	28.5	23
		Slope	0.8		
		Depth	0.9		
		Dist coast	3.0		

Table 5. Model description and diagnostics for the final selected models of **bottlenose dolphin** individuals in SCANS-III (2016) and SCANS-II/CODA (2005/07). Covariates in the models are described in Table 1.

Dataset	Error distribution	Model covariates	Estimated degrees of freedom	Model degrees of freedom	% Deviance explained
SCANS-III (2016)	Negative binomial	X, Y	7.8	9.5	38
		CS 50	0.8		
SCANS-II and CODA (2005/07)	Negative binomial	X, Y	1.9	4.5	28
		Depth	0.8		
		ADT	0.8		

Table 6. Model description and diagnostics for the final selected models of **white-beaked dolphin** individuals in SCANS-III (2016) and SCANS-II/CODA (2005/07). Covariates in the models are described in Table 1.

Dataset	Error distribution	Model covariates	Estimated degrees of freedom	Model degrees of freedom	% Deviance explained
SCANS-III (2016)	Tweedie	X, Y	12.1	19.5	56
		SST	0.7		
		Dist 200	5.8		
SCANS-II and CODA (2005/07)	Tweedie	X, Y	11.2	16.3	55
		Depth	0.8		
		Aspect	3.4		

Table 7. Model description and diagnostics for the final selected models of **common dolphin** groups in SCANS-III (2016) and SCANS-II/CODA (2005/07). Covariates in the models are described in Table 1.

Dataset	Error distribution	Model covariates	Estimated degrees of freedom	Model degrees of freedom	% Deviance explained
SCANS-III (2016)	Negative binomial	X, Y	12.7	19.0	64
		Depth	1.0		
		Slope	2.5		
		Aspect	1.8		
SCANS-II and CODA (2005/07)	Negative binomial	X, Y	15.6	21.6	43
		SLA	4.0		
		Slope	0.9		

Table 8. Model description and diagnostics for the final selected models of **striped dolphin** groups in SCANS-III (2016) and SCANS-II/CODA (2005/07). Covariates in the models are described in Table 1.

Dataset	Error distribution	Model covariates	Estimated degrees of freedom	Model degrees of freedom	% Deviance explained
SCANS-III (2016)	Negative binomial	X, Y	1.8	7.9	40
		Depth	3.1		
		Depth SD	0.9		
		Aspect	1.2		
SCANS-II and CODA (2005/07)	Negative binomial	X, Y	1.7	5.5	48
		Depth	2.2		
		Dist 200	0.5		

Table 9. Model description and diagnostics for the final selected models of **common and striped dolphins, including unidentified common or striped dolphins** groups in SCANS-III (2016) and SCANS-II/CODA (2005/07). Covariates in the models are described in Table 1.

Dataset	Error distribution	Model covariates	Estimated degrees of freedom	Model degrees of freedom	% Deviance explained
SCANS-III (2016)	Negative binomial	X, Y	15.2	21.0	61
		Depth	1.0		
		Depth SD	0.9		
		Aspect	2.4		
		Dist 2000	0.5		
SCANS-II and CODA (2005/07)	Negative binomial	X, Y	16.2	22.5	44
		Depth	0.9		
		SLA	3.5		
		Depth SD	0.9		

Table 10. Model description and diagnostics for the final selected models of **pilot whale** individuals in SCANS-III (2016) and SCANS-II/CODA (2005/07). Covariates in the models are described in Table 1.

Dataset	Error distribution	Model covariates	Estimated degrees of freedom	Model degrees of freedom	% Deviance explained
SCANS-III (2016)	Tweedie	X, Y	13.9	17.3	59
		Depth SD	2.4		
SCANS-II and CODA (2005/07)	Tweedie	X, Y	1.8	6.4	53
		ADT	0.7		
		Depth SD	0.8		
		Aspect	1.1		
		Dist 2000	1.0		

Table 11. Model description and diagnostics for the final selected models of **beaked whales (all species combined)** individuals in SCANS-III (2016) and SCANS-II/CODA (2005/07). Covariates in the models are described in Table 1.

Dataset	Error distribution	Model covariates	Estimated degrees of freedom	Model degrees of freedom	% Deviance explained
SCANS-III (2016)	Negative binomial	Depth	4.8	6.3	51
		SST	0.6		
SCANS-II and CODA (2005/07)	Tweedie	X, Y	10.1	14.2	65
		Depth SD	2.1		
		Depth	0.9		

Table 12. Model description and diagnostics for the final selected models of **fin whale** individuals in SCANS-III (2016) and SCANS-II/CODA (2005/07). Covariates in the models are described in Table 1.

Dataset	Error distribution	Model covariates	Estimated degrees of freedom	Model degrees of freedom	% Deviance explained
SCANS-III (2016)	Negative binomial	X, Y	9.9	14.8	71
		CS 200	3.9		
SCANS-II and CODA (2005/07)	Negative binomial	X, Y	11.4	19.9	68
		Depth SD	0.8		
		Dist 50	6.8		

Table 13. Model description and diagnostics for the final selected models of **minke whale** individuals in SCANS-III (2016) and SCANS-II/CODA (2005/07). Covariates in the models are described in Table 1.

Dataset	Error distribution	Model covariates	Estimated degrees of freedom	Model degrees of freedom	% Deviance explained
SCANS-III (2016)	Negative binomial	X, Y	6.9	10.5	24
		Depth	0.9		
		ADT	0.8		
		Dist coast	0.9		
SCANS-II and CODA (2005/07)	Negative binomial	X, Y	15.1	18.9	39
		Depth SD	0.8		
		Aspect	1.0		
		Dist 2000	0.6		

Maps showing surfaces of predicted density and estimated coefficient of variation (CV) of predicted density are shown for each species for SCANS-III (2016) and for SCANS-II/CODA (2005/07) in Figures 3-12. For harbour porpoise, the maps are for SCANS-III and SCANS-II (Figure 3). For each species, the density surface maps are plotted on the same scale for 2016 and 2005/07. The maps thus illustrate between-year differences in overall density/abundance as well as variation in predicted distribution. The patterns of predicted density are influenced by the covariates retained in the models (see Tables 4-12), the fitted smooth functions (see Appendices A.2 and A.3), and spatial variation in the values of the covariates in the prediction grid.

The maps of CVs provide a measure of the confidence in predicted density across the survey area. Lower CVs are generally associated with areas of higher density. Confidence in the predictions in areas of low density is generally much poorer. The magnitude of the CVs is influenced by the number of sightings as well as by how well the models fit the data. Thus, the CVs for predicted harbour porpoise density (Figure 3) are relatively low across most of the survey area because of the much larger number of sightings, despite the fact that the models explained less deviance for porpoises than for other species (Table 4).

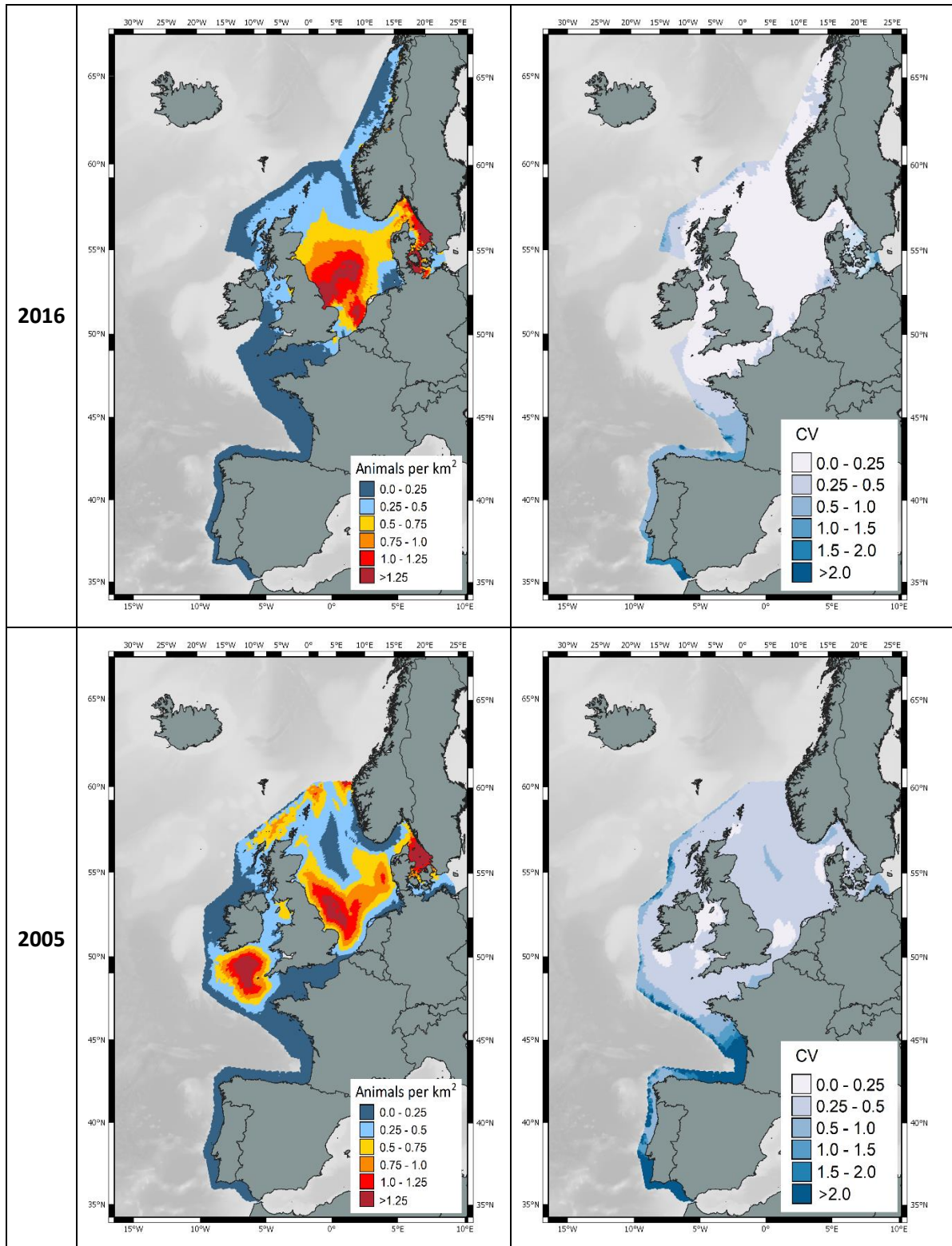


Figure 3. Predicted surfaces of estimated density [left] and associated coefficient of variation (CV) [right] for harbour porpoise in SCANS-III (2016) [top] and SCANS-II (2005) [bottom].

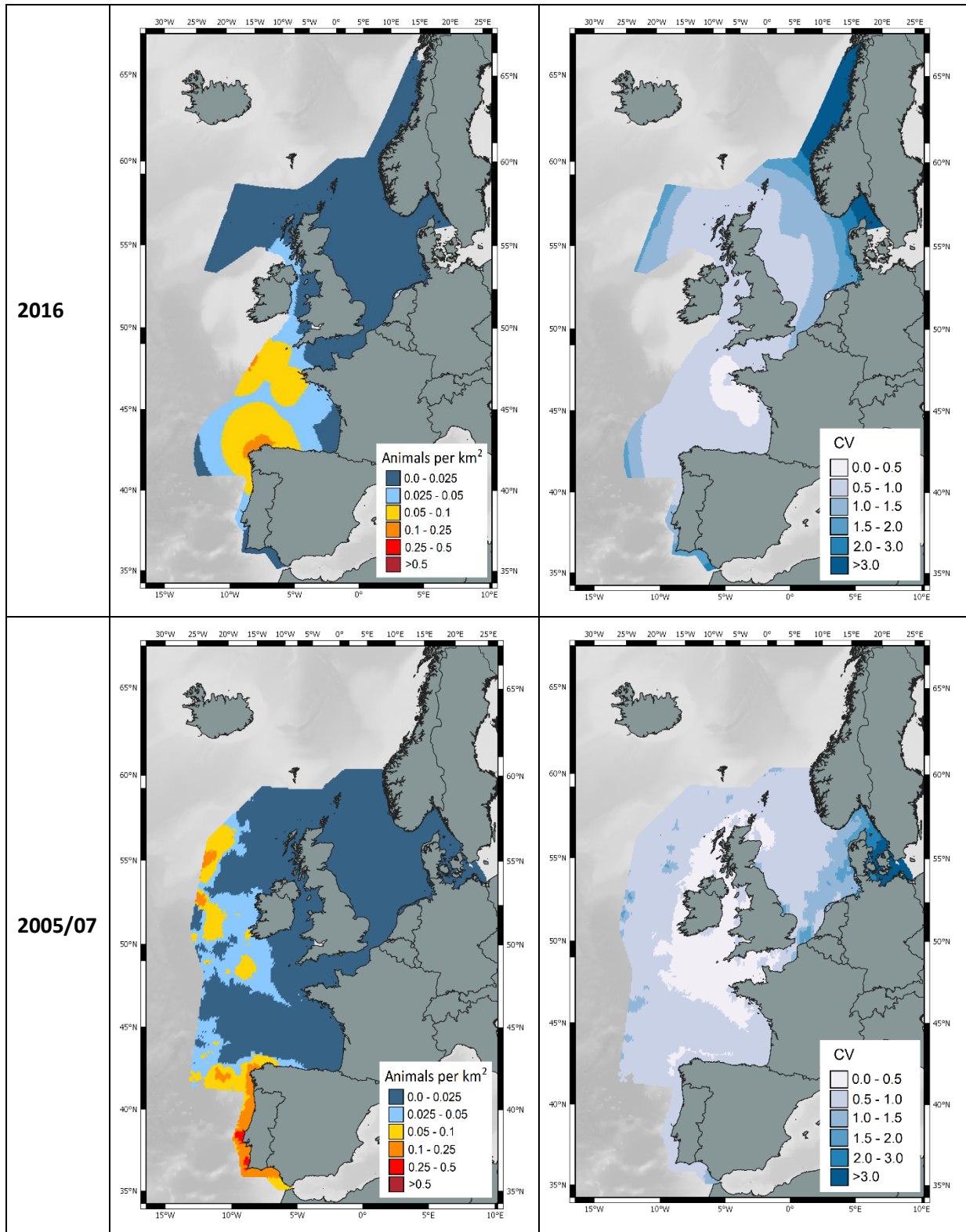


Figure 4. Predicted surfaces of estimated density [left] and associated coefficient of variation (CV) [right] for **bottlenose dolphin** in SCANS-III (2016) [top] and SCANS-II/CODA (2005/07) [bottom].

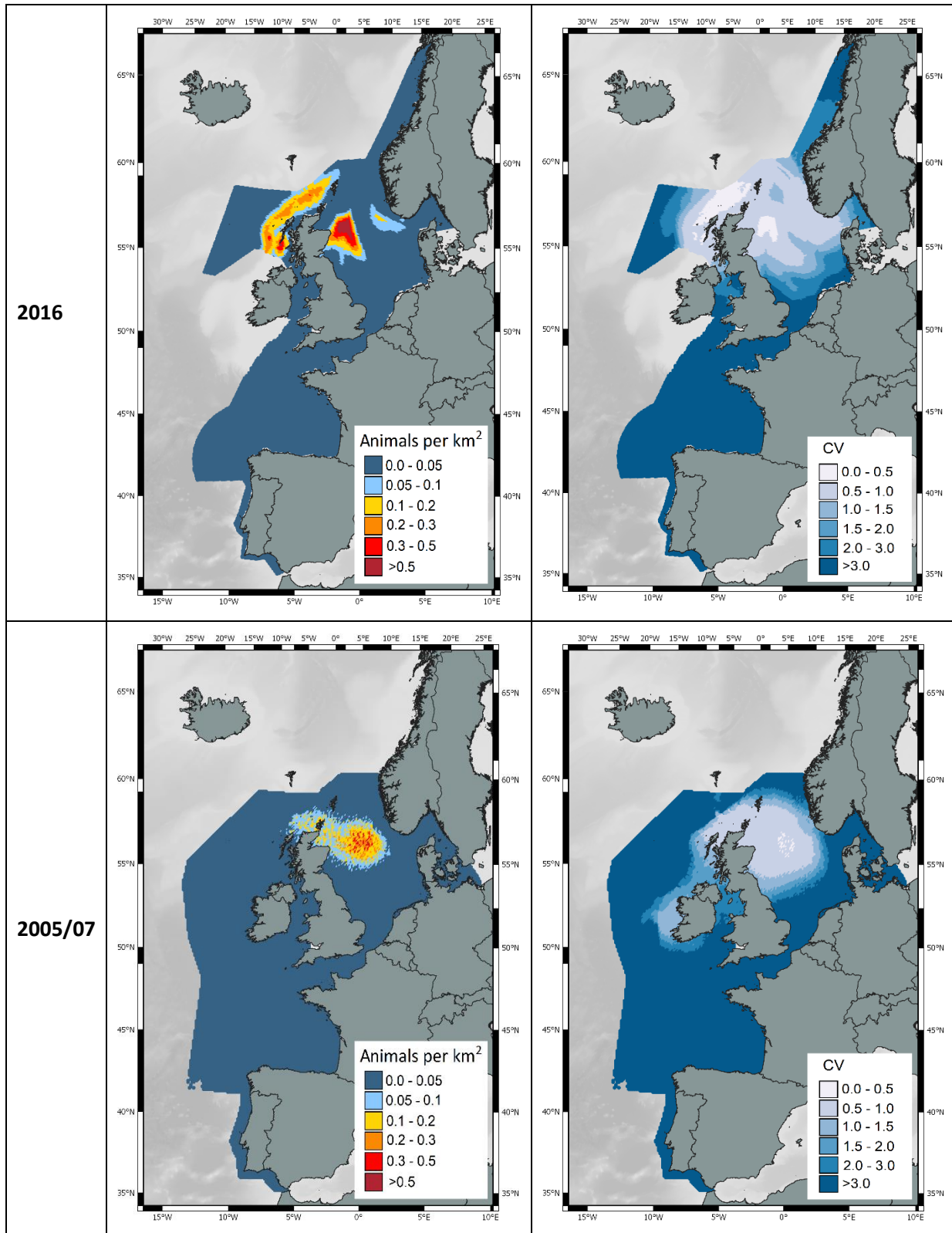


Figure 5. Predicted surfaces of estimated density [left] and associated coefficient of variation (CV) [right] for **white-beaked dolphin** in SCANS-III (2016) [top] and SCANS-II/CODA (2005/07) [bottom].

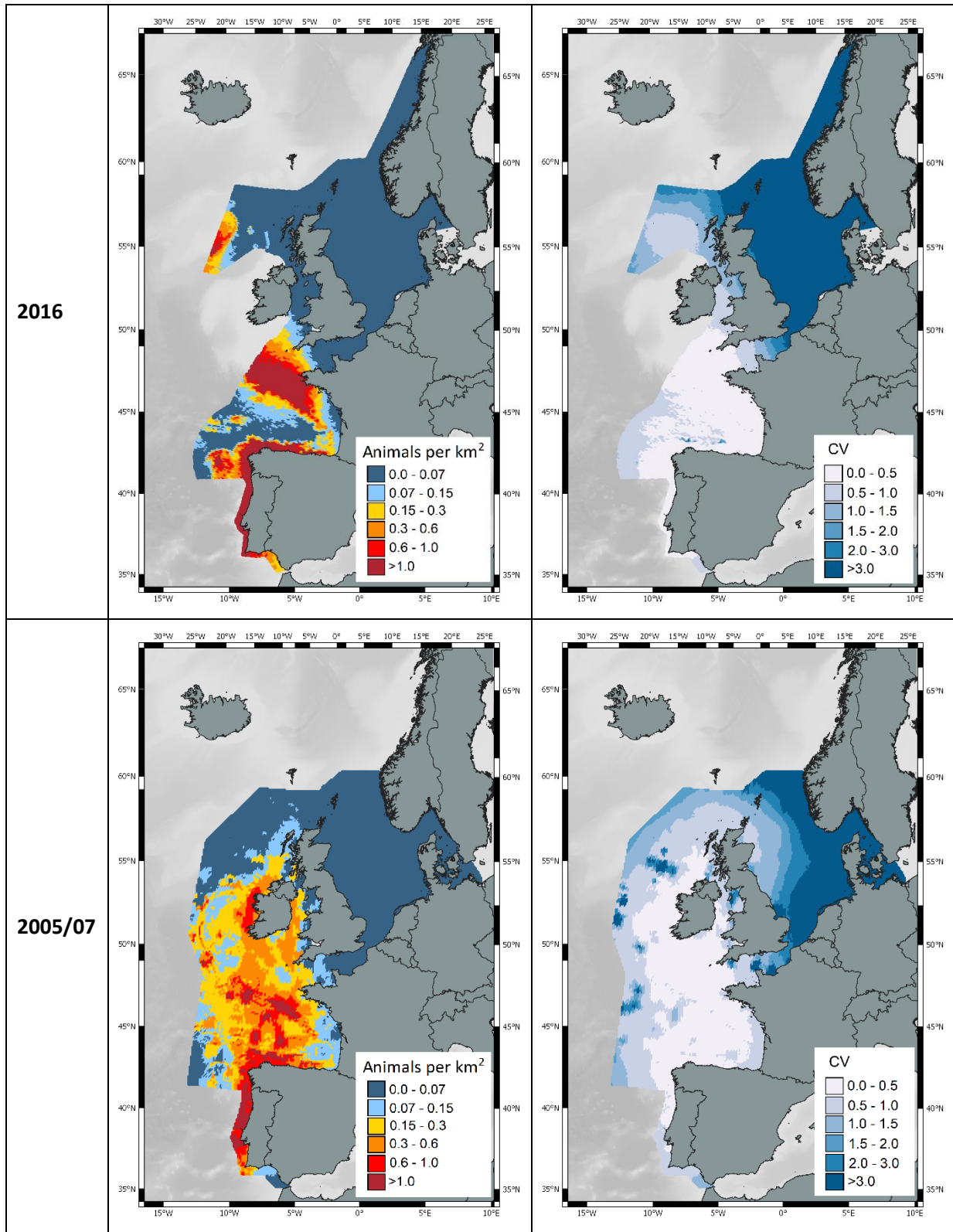


Figure 6. Predicted surfaces of estimated density [left] and associated coefficient of variation (CV) [right] for **common dolphin** in SCANS-III (2016) [top] and SCANS-II/CODA (2005/07) [bottom].

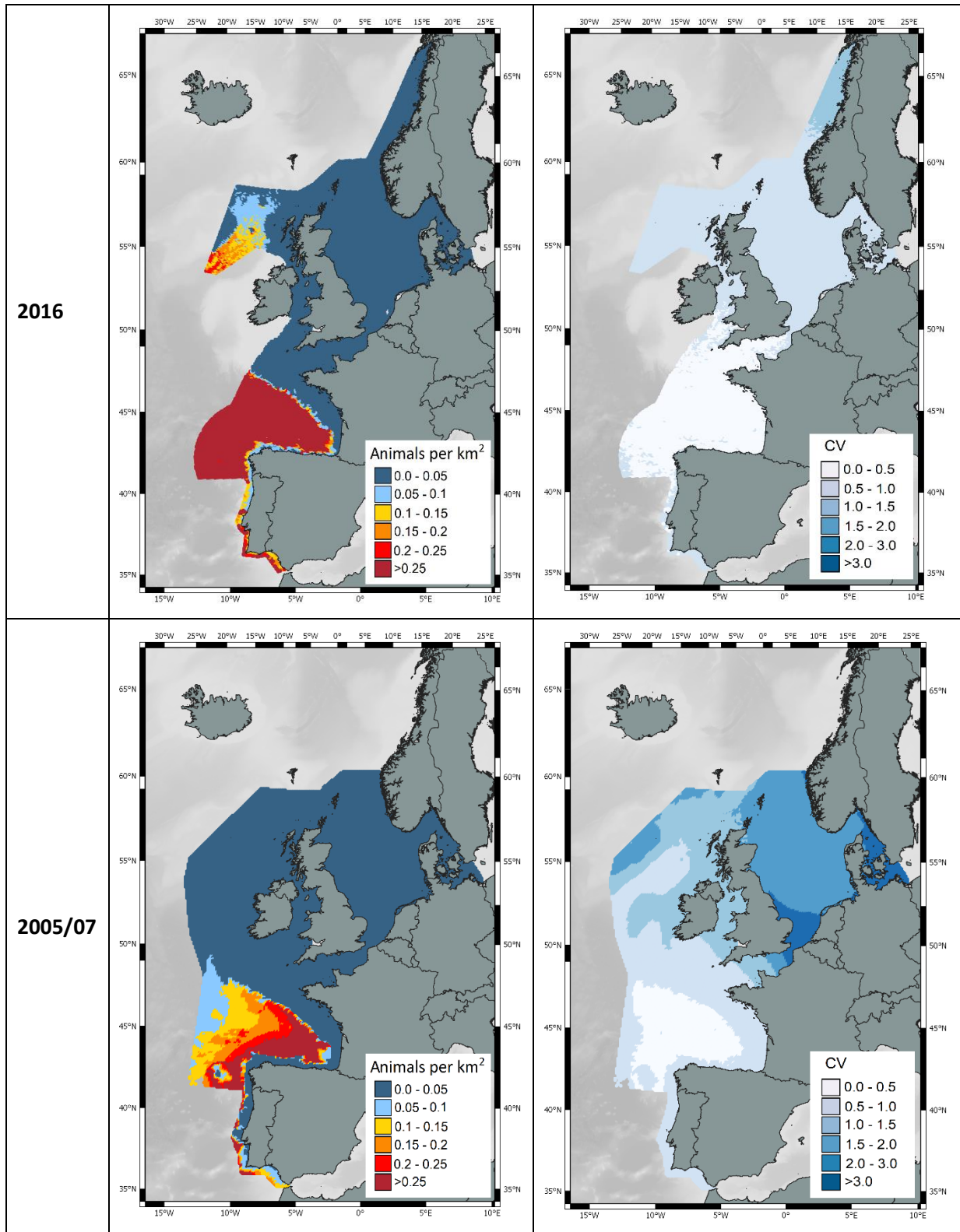


Figure 7. Predicted surfaces of estimated density [left] and associated coefficient of variation (CV) [right] for striped dolphin in SCANS-III (2016) [top] and SCANS-II/CODA (2005/07) [bottom].

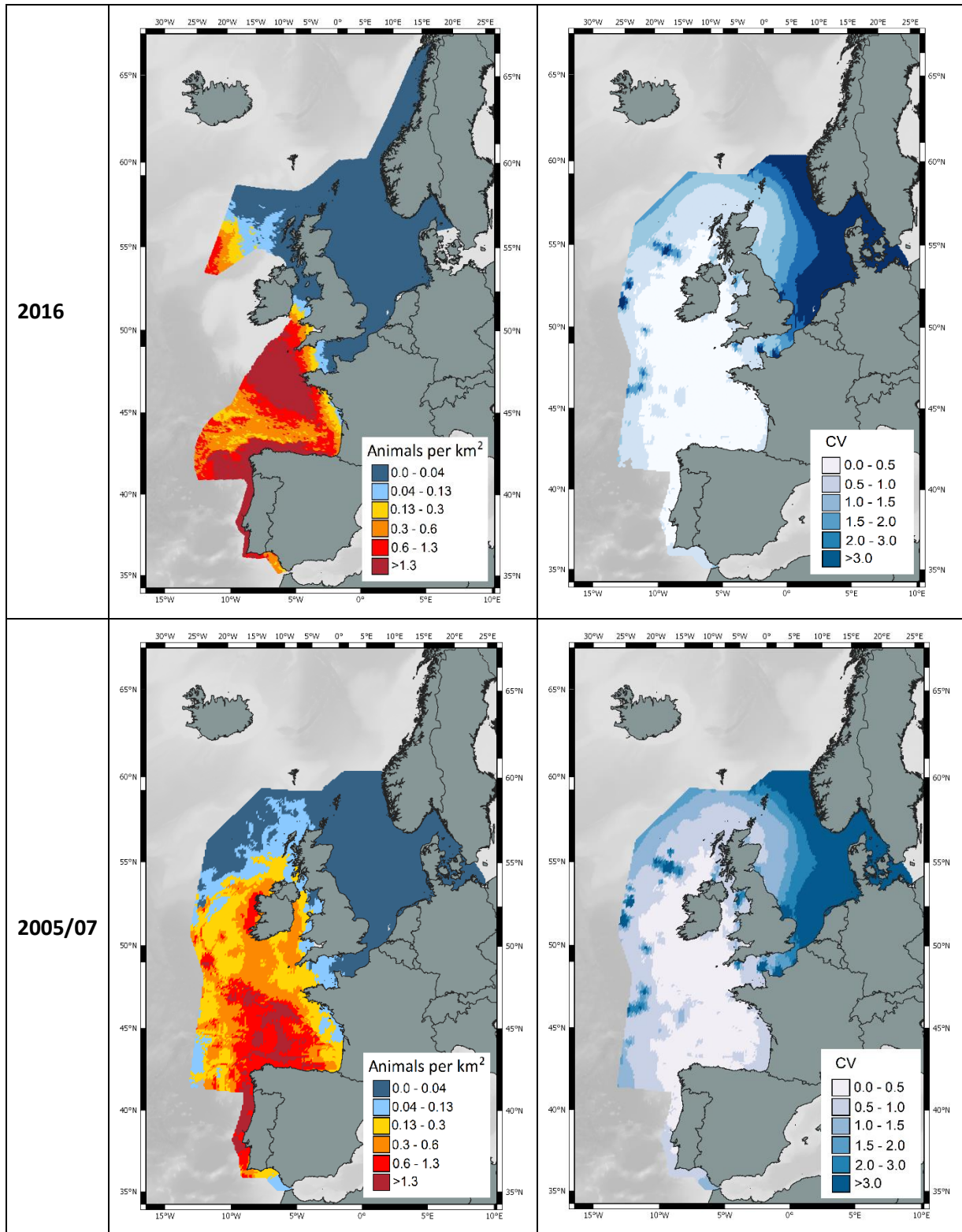


Figure 8. Predicted surfaces of estimated density [left] and associated coefficient of variation (CV) [right] for common and striped dolphins, including unidentified common or striped dolphins in SCANS-III (2016) [top] and SCANS-II/CODA (2005/07) [bottom].

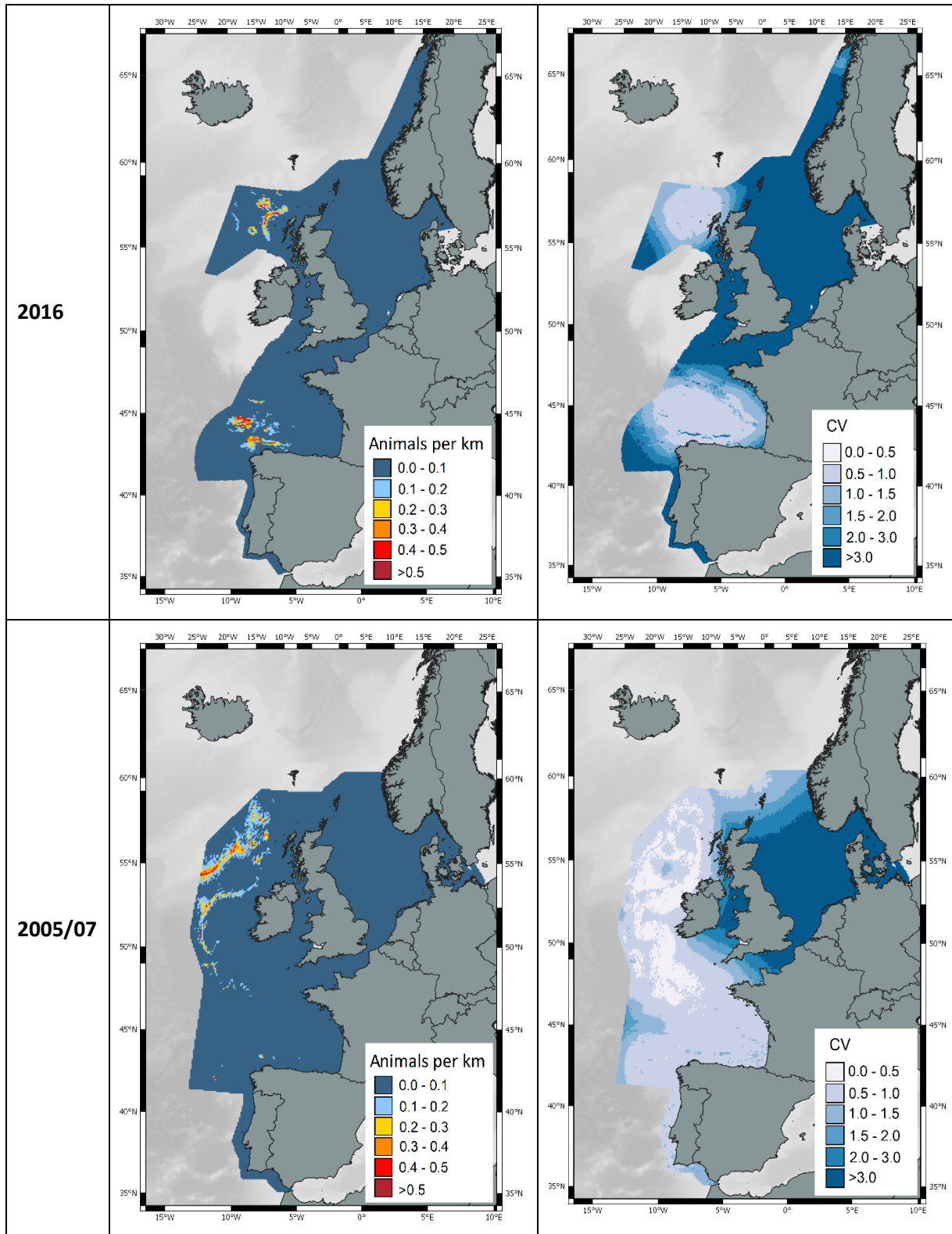


Figure 9. Predicted surfaces of estimated density [left] and associated coefficient of variation (CV) [right] for pilot whale in SCANS-III (2016) [top] and SCANS-II/CODA (2005/07) [bottom].

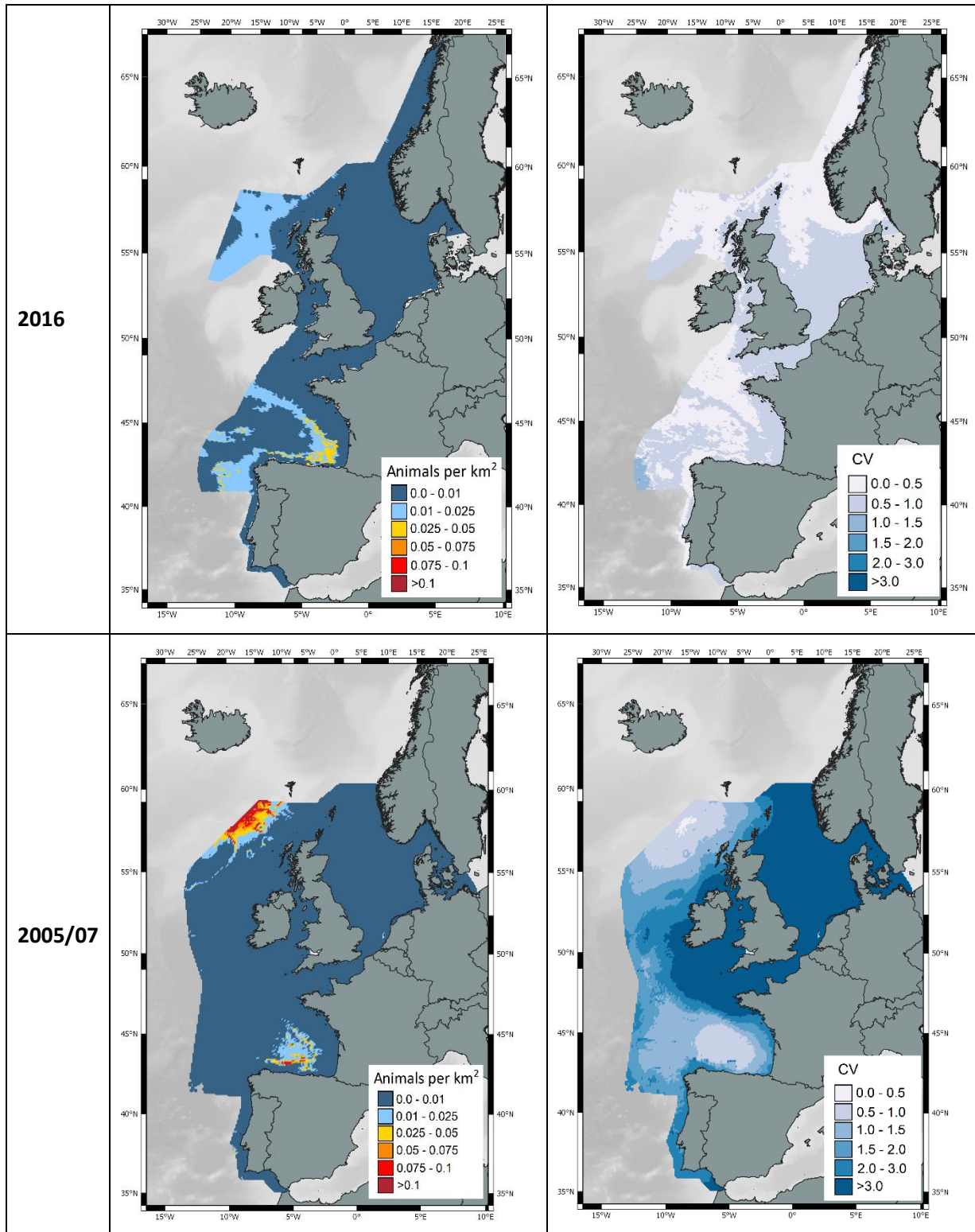


Figure 10. Predicted surfaces of estimated density [left] and associated coefficient of variation (CV) [right] for **beaked whales (all species combined)** in SCANS-III (2016) [top] and SCANS-II/CODA (2005/07) [bottom].

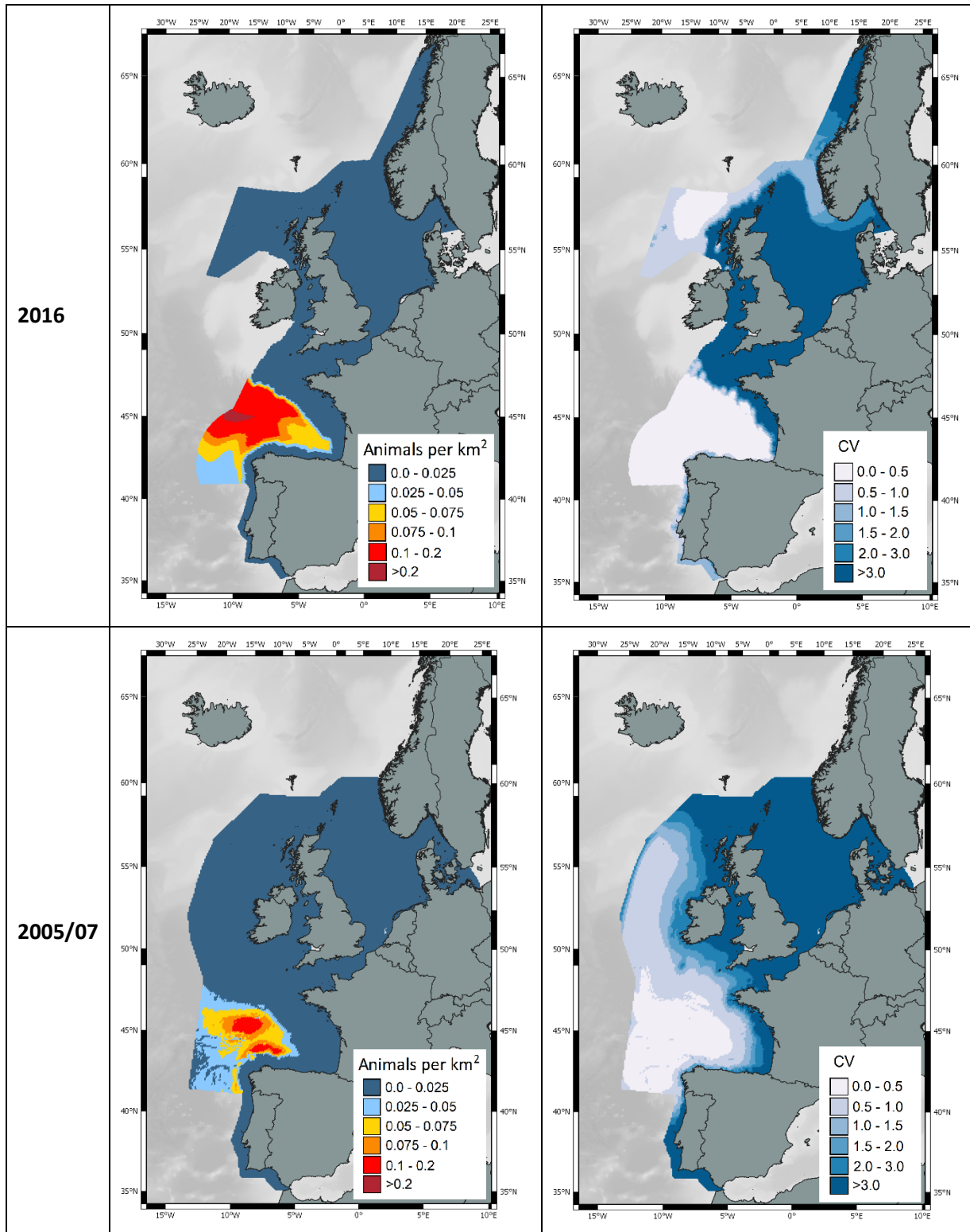


Figure 11. Predicted surfaces of estimated density [left] and associated coefficient of variation (CV) [right] for fin whale in SCANS-III (2016) [top] and SCANS-II/CODA (2005/07) [bottom].

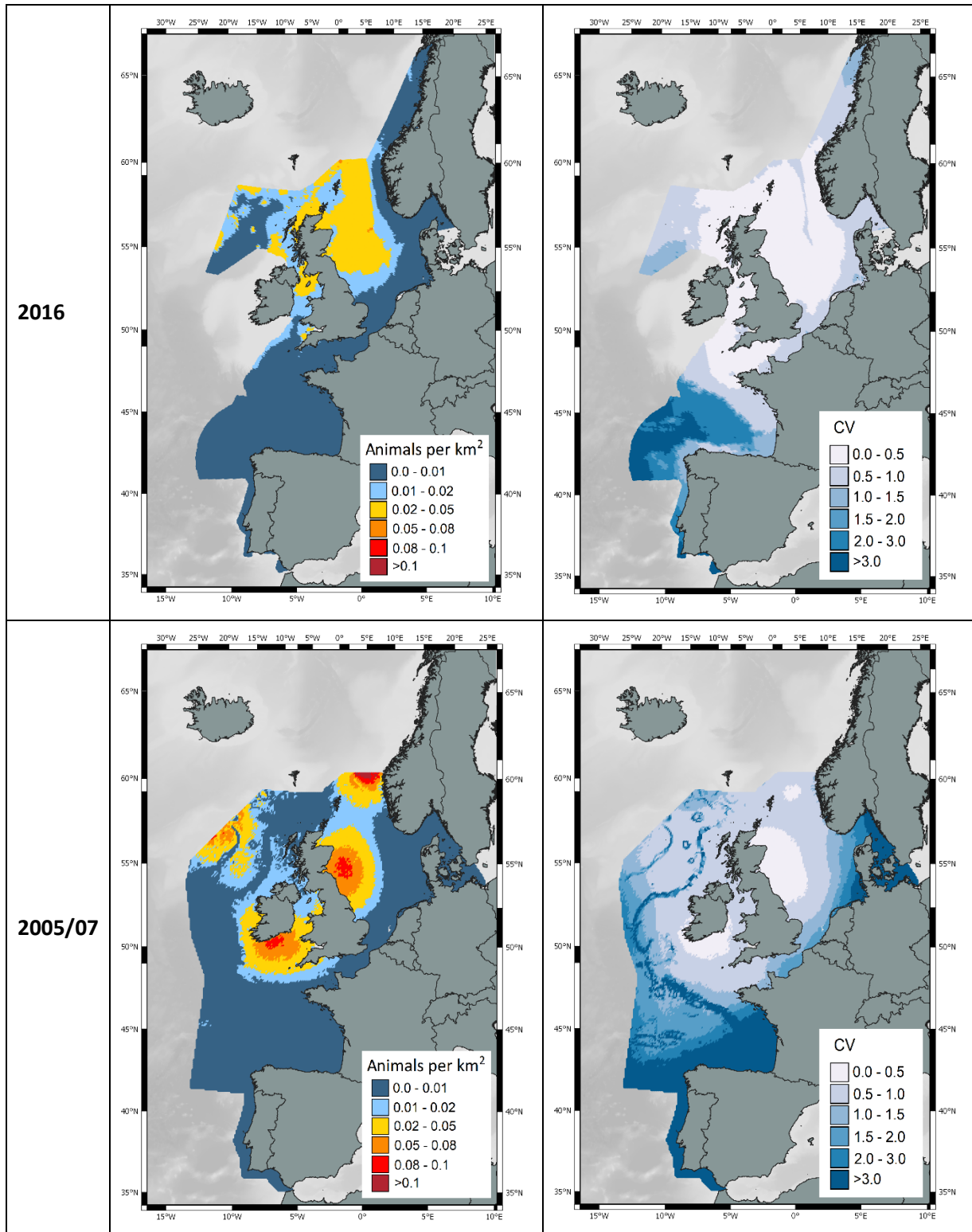


Figure 12. Predicted surfaces of estimated density [left] and associated coefficient of variation (CV) [right] for minke whale in SCANS-III (2016) [top] and SCANS-II/CODA (2005/07) [bottom].

DISCUSSION

Harbour porpoise

A marked shift in the distribution of harbour porpoise in the North Sea from north to south was previously detected between 1994 and 2005 (Hammond et al., 2013). Results from the current analysis indicate that the predicted distribution in 2016 in the North Sea is quite similar to that in 2005 (Figure 3). There is some indication that the distribution of porpoises in 2016 extended slightly further into the eastern part of the English Channel than in 2005; however, predicted density in the English Channel overall is still low, as discussed by Hammond et al. (2021).

The most noticeable difference between the modelled distributions is that the high density predicted in the Celtic Sea (southwest of Britain and Ireland) in 2005 is not predicted in 2016 (Fig 3). However, part of the Celtic Sea was surveyed by ObSERVE instead of SCANS-III in 2016 (see Fig 1) and high densities of harbour porpoise were predicted in this area in the summers of 2015 and 2016 (Rogan et al. 2018). In addition, high harbour porpoise density was predicted to the west of Ireland (Rogan et al. 2018). One explanation for the lower predicted density of harbour porpoises in the Celtic Sea in SCANS-III in 2016 could therefore be a distributional shift into Irish waters covered by the ObSERVE surveys.

Gilles et al. (2016) generated density surface maps of harbour porpoise in the North Sea from systematic surveys in German, Danish, Dutch and Belgian waters and on the Dogger Bank. These predictions cover the period 2005-2013 and include data from SCANS-II. The distribution presented here for SCANS-III (Figure 3) is rather similar to the map for summer from Gilles et al. (2016) but extending further south. Densities modelled from the SAMM 2012 summer survey showed higher densities in the southern North Sea and the Eastern Channel than in the western Channel and Celtic Plateau (Lambert et al., 2017).

Bottlenose dolphin

The modelled distribution of bottlenose dolphins in 2016 shows the highest predicted densities in the Celtic Sea and Bay of Biscay, particularly off the coast of Galicia (NW Spain) (Figure 4). The modelled distribution in 2005/07 shows similar predicted densities in the same areas but also to the west of Ireland and higher densities along the Portuguese coast (Figure 4). New information for summer 2016 in Irish waters shows high predicted densities off the southwest and west coast of Ireland and also further offshore to the southwest in deeper waters (Rogan et al., 2018). There are therefore similarities in the distribution of bottlenose dolphins between 2005/07 and 2016 but also some differences, particularly the high densities predicted around the coast of Portugal in 2016.

Densities predicted from the SAMM surveys in 2011 and 2012 indicated high-density areas along the Atlantic continental slope and in oceanic water north-west of the Iberian Peninsula (Lambert et al., 2017).

Small, coastal populations of bottlenose dolphins exist in Ireland, the UK, France, Spain and Portugal (see ICES 2016). Large scale line transect surveys such as SCANS, ObSERVE and SAMM are not designed to collect data at a sufficiently small spatial scale necessary to generate estimates of abundance from these small, coastal populations. The appropriate method to obtain abundance estimates for these populations is mark-recapture analysis of photo-identification data (e.g., Arso Civil et al., 2019).

White-beaked dolphin

The modelled distribution of white-beaked dolphins in 2016 shows predicted high density areas in the northern North Sea to the east of Scotland and to the north and west of Scotland, very similar to the predicted distribution in 2005/07 from the SCANS-II/CODA surveys (Figure 5). This pattern is also reflected in the distribution of sightings in the North Sea in 1994 from the SCANS survey (Hammond et al., 2002).

The ObSERVE surveys in Irish waters in 2015-17 recorded few white-beaked dolphin sightings (22 in total), and mostly in summer. A few were recorded off the west coast of Ireland, but most were distributed further west along the shelf edge or on the Porcupine Bank (Rogan et al., 2018).

The North Atlantic Sighting Survey (NASS) in 2015 recorded no white-beaked dolphins in the Faroes blocks (Figure 1; Pike et al., 2019).

Common and striped dolphins

The modelled distribution of common dolphins in 2016 shows high predicted density in shelf waters and along the shelf edge in the northern Bay of Biscay and Celtic Sea and around the coasts of Spain and Portugal (Figure 6). There are also predicted high density areas to the west of Galicia (NW Spain) and on the westernmost edge of the survey area west of Scotland. The ObSERVE surveys in Irish waters in 2015-17 recorded common dolphins mostly in winter; the summer sightings were distributed throughout shelf waters to the west of Ireland in 2015 but were highly concentrated off the southwest coast in 2016 (Rogan et al., 2018). This pattern is quite similar to the predicted distribution in 2005/07 from SCANS-II/CODA, except that in those earlier years predicted density was lower in shelf waters in the northern Bay of Biscay and Celtic Sea but higher in deep waters in the Bay of Biscay (Figure 6).

The NASS in 2015 recorded several sightings of common dolphins in the southern-most part of the Faroes blocks west of Ireland (Figure 1; Pike et al., 2019).

In 2016, the predicted distribution of striped dolphins shows high densities in waters off the shelf throughout the Bay of Biscay and west of Galicia (NW Spain) (Figure 7). This distribution is thus largely disjunct from that of common dolphins, except that there is overlap in predicted high density of the two species along the shelf edge of the Bay of Biscay and west of Galicia (NW Spain). The predicted high density area of striped dolphins in deep waters west of Scotland (Figure 7) is east of, and thus also disjunct from, the adjacent area of predicted high common dolphin density (Figure 6). No robust model prediction for striped dolphins could be obtained for 2005/07.

The modelled distributions of common and striped dolphins, including those sightings recorded as either common or striped, largely reflect those of common dolphins, driven by the much greater number of sightings of that species (Figure 8; Tables 2, 3).

The pattern of sightings and predicted distributions of common and striped dolphins in summer 2012 from the French SAMM surveys in the Bay of Biscay are similar to those described above (Laran et al., 2017, Lambert et al., 2017).

Long-finned pilot whale

The modelled distribution of pilot whales in 2016 shows predicted high-density areas off the shelf edge west of Scotland, and in deep waters in the southern Bay of Biscay (Figure 9). This distribution is somewhat similar to that predicted in 2005/07 from the SCANS-II and CODA survey data (see also Rogan et al., 2017), and in the SAMM survey (pilot whale and Risso's dolphin analysed jointly; Lambert et al., 2017), but there were higher predicted densities in the Bay of Biscay in 2016 than in 2005/07 (Figure 9).

The ObSERVE surveys in 2015-17 show high predicted densities of pilot whales in summer along the length of the continental shelf to the west of Ireland (similar to the pattern seen in CODA 2007; Figure 9) and also in deeper waters, especially to the north of the survey area (Rogan et al., 2018).

More than 60 sightings of pilot whales were made throughout the Faroes blocks of the NASS in summer 2015, from north of Scotland to west of Ireland (Figure 1; Pike et al., 2019).

Beaked whales (all species)

The modelled distribution of beaked whales (all species) in 2016 shows the highest predicted density off the north coast of Spain, west of Galicia, in the south-eastern Bay of Biscay, along the shelf edge in the northern Bay of Biscay, and in deep waters west of Scotland (Figure 10). This predicted distribution in 2016 is similar to that in 2005/07 (Figure 10; Rogan et al., 2017) except that predicted density was higher west of Scotland in 2007. These predicted distributions also reflect the distribution of opportunistic sightings of beaked whales (ICES 2016).

The ObSERVE surveys in Irish waters recorded several species of beaked whale in 2015-17 in winter and summer, almost all in deep waters off the continental shelf (Rogan et al., 2018).

Almost 40 sightings of northern bottlenose whales were made in the Faroes blocks of the NASS in summer 2015, mostly in the northern block (Figure 1; Pike et al., 2019).

Fin whale

The predicted distributions of fin whales in 2016 and in 2005/07 are very similar, showing high predicted densities in offshore waters of the Bay of Biscay (Figure 11). This species showed the least variation in predicted distribution between the surveys in 2005/07 and 2016 of any of the species modelled.

Most sightings of fin whales in the ObSERVE surveys were in winter with very few sightings made in summer 2016 (Rogan et al., 2018). However, around 100 sightings of fin whales were made throughout the Faroes blocks of the NASS in summer 2015, from north of Scotland to west of Ireland (Figure 1; Pike et al., 2019).

Minke whale

The predicted distribution of minke whales in 2016 shows the highest density across the central and north-eastern North Sea, and in shelf waters west of Scotland (Figure 12). In 2005/07, the predicted distribution is similar in the North Sea but also shows high density in the Celtic Sea (Figure 12), a pattern reflected in the sightings of minke whales in the SCANS survey in 1994 (Hammond et al., 2002). In both 2005/07 and 2016, there are areas of high predicted density towards the western edge of the survey area west of Scotland (Figure 12).

More than 40 sightings of minke whales were made throughout the Faroes blocks of the NASS in summer 2015, from north of Scotland to west of Ireland (Figure 1; Pike et al., 2019).

CONCLUDING REMARKS

In this report, we present the results of density surface modelling of data from the third in a time series (1994, 2005/07, 2016) of large-scale multinational surveys of cetaceans in European Atlantic waters. This third survey, SCANS-III, includes all European Atlantic waters except for Portuguese offshore waters, which remain largely unsurveyed, and waters to the south and west of Ireland, which were surveyed in 2015-17 as part of the ObSERVE project (Rogan et al., 2018). For comparison, we also present equivalent results from revised analyses from the SCANS-II and CODA surveys in 2005/07 (Hammond et al., 2013; CODA, 2009; Rogan et al., 2017). For some species, we can also compare these results with information from the SCANS survey in 1994 (Hammond et al., 2002) and from other large-scale, systematic surveys in the same area (Gilles et al., 2016; Lambert et al., 2017; Rogan et al., 2018).

For most of the species encountered in the SCANS surveys, the survey area is at the eastern edge of their broad North Atlantic range. It is thus expected that their distribution and abundance in European Atlantic waters could be influenced by environmental conditions and prey availability in the wider North Atlantic as well as by conditions European Atlantic waters. The series of SCANS surveys is designed to monitor decadal-scale changes but prey availability in the area is likely to vary inter-annually and thus influence cetacean distribution and/or abundance in the area. Results from the ObSERVE surveys showed inter-annual variability between 2015 and 2016 for some species (Rogan et al., 2018). SCANS surveys always take place in summer to take advantage of more favourable survey conditions and to ensure comparability across the series. Prey availability, and therefore cetacean distribution and/or abundance, may also vary seasonally and this may explain differences between winter and summer in predicted distributions of several species in Irish waters (Rogan et al., 2018).

Nevertheless, the distributions of the most abundant species of cetacean in European Atlantic waters in 2016 predicted from the SCANS-III survey, supported by results from the ObSERVE surveys in Irish waters in 2015/17, are broadly similar to those predicted from the SCANS-II and CODA surveys in 2005/07 (Figures 3-12). We did not find evidence for much change in cetacean distribution between 2005 and 2016, despite well-documented environmental changes in European Atlantic waters in recent decades (e.g., Heath, 2005; Brander et al., 2016; Capuzzo et al., 2017 for the North Sea).

However, ongoing directional changes in ocean conditions are expected as a result of climate warming. It is therefore important to continue monitoring cetacean distribution to inform the status of species and the wider environment.

The predicted densities from density surface modelling can be used to generate abundance estimates for the entire survey area or a defined area within it. For the entire survey area, we found that these model-based estimates were mostly within around 10% of the design-based estimates (Hammond et al., 2021) but for two species, striped dolphin and fin whale, the difference was around 20%. Taking into account the uncertainty around the estimates (CVs mostly between 0.25 and 0.45), and that the model-based estimates are predicted from a model fitted to data over a large and ecologically diverse study area, the

model-based estimates reflect the design-based estimates quite well. The best estimates for the entire study area are the design-based estimates presented in Hammond et al. (2021).

ACKNOWLEDGEMENTS

Covariate data on Absolute Dynamic Topography (ADT), Sea Level Anomaly (SLA) and Sea Surface Temperature (SST) were provided by NEODAAS, the NERC Earth Observation Data Acquisition and Analysis Service (<https://www.neodaas.ac.uk/>).

REFERENCES

- Amante, C. & Eakins, BW (2009). ETOPO1 1 Arc-Minute Global Relief Model: Procedures, Data Sources and Analysis. NOAA Technical Memorandum NESDIS NGDC-24, 19 pp.
- Becker, EA, Forney, KA, Fiedler, PC, Barlow, J, Chivers, SJ, Edwards, CA, Moore, AM & Redfern, JV (2016). Moving towards dynamic ocean management: how well do modeled ocean products predict species distributions? *Remote Sensing* 8: 149. doi: 10.3390/rs8020149
- Becker, EA, Forney, KA, Thayre, BJ, Debich, AJ, Campbell, GS, Whitaker, K, Douglas, AB, Gilles, A, Hoopes, R & Hildebrand, JA (2017). Habitat-based density models for three cetacean species off Southern California illustrate pronounced seasonal differences. *Frontiers in Marine Science* 4: 121. doi: 10.3389/fmars.2017.00121
- Brander, KM, Ottersen, G, Bakker, JP, Beaugrand, G, Herr, H, Garthe, S, Gilles, A, Kenny, A, Siebert, U, Skjoldal, HR & Tulp, I (2016). Environmental impacts – marine ecosystems. In: Quante, M & Colijn, F (eds) *North Sea Region Climate Change Assessment*. Springer Nature. doi: 10.1007/978-3-319-39745-0
- Capuzzo, E, Lynam, CP, Barry, J, Stephens, D, Forster, RM, Greenwood, N, McQuatters-Gollop, A, Silva, T, van Leeuwen, SM, & Engelhard, GH (2018). A decline in primary production in the North Sea over 25 years, associated with reductions in zooplankton abundance and fish stock recruitment. *Global Change Biology*, 24: e352-e364. <https://doi.org/10.1111/gcb.13916>
- CODA (2009). *Cetacean Offshore Distribution and Abundance in the European Atlantic (CODA)*. Final Report. University of St Andrews, UK. <http://biology.st-andrews.ac.uk/coda/>.
- Gilles, A, Viquerat, S, Becker, EA, Forney, KA, Geelhoed, SCV, Haelters, J, Nabe-Nielsen, J, Scheidat, M, Siebert, U, Sveegaard, S, van Beest, FM, van Bemmelen, R, Aarts, G (2016). Seasonal habitat-based density models for a marine top predator, the harbor porpoise, in a dynamic environment. *Ecosphere* 7(6): e01367. doi: 10.1002/ecs2.1367
- QGIS (2021). QGIS Geographic Information System. QGIS Association. <http://www.qgis.org>.
- Hammond, PS, Berggren, P, Benke, H, Borchers, DL, Collet, A, Heide-Jørgensen, MP, Heimlich, S, Hiby, AR, Leopold, MF & Øien, N (2002). Abundance of harbour porpoises and other cetaceans in the North Sea and adjacent waters. *Journal of Applied Ecology* 39: 361-376.
- Hammond, PS, Macleod, K, Berggren, P, Borchers, DL, Burt, ML, Cañadas, A, Desportes, G, Donovan, GP, Gilles, A, Gillespie, D, Gordon, J, Hiby, L, Kuklik, I, Leaper, R, Lehnert, K, Leopold, M, Lovell, P, Øien, N, Paxton, CGM, Ridoux, V, Rogan, E, Samarra, F, Scheidat, M, Sequeira, M, Siebert, U, Skov, H, Swift, R, Tasker, ML, Teilmann, J, Van Canneyt, O & Vázquez, JA. (2013). Cetacean abundance and distribution in

European Atlantic shelf waters to inform conservation and management. *Biological Conservation* 164: 107-122. doi: 10.1016/j.biocon.2013.04.010

Hammond, PS, Lacey, C, Gilles, A, Viquerat, S, Börjesson, P, Herr, H, Macleod, K, Ridoux, V, Santos, MB, Scheidat, M, Teilmann, J, Vingada, J & Øien, N (2021). Estimates of cetacean abundance in European Atlantic waters in summer 2016 from the SCANS-III aerial and shipboard surveys. SCANS-III project report 1, 41pp. https://scans3.wp.st-andrews.ac.uk/files/2021/06/SCANS-III_design-based_estimates_final_report_revised_June_2021.pdf.

Heath, MR (2005). Changes in the structure and function of the North Sea fish foodweb, 1973–2000, and the impacts of fishing and climate. *ICES Journal of Marine Science* 62: 847-868. <https://doi.org/10.1016/j.icesjms.2005.01.023>

ICES (2016). Report of the Working Group on Marine Mammal Ecology (WGMME), 8-11 February 2016, Madrid, Spain. ICES CM 2016/ACOM: 26.

Lambert, C, Pettex, E, Dorémus, G, Laran, S, Stéphan, E, Van Canneyt, O & Ridoux, V (2017). How does ocean seasonality drive habitat preferences of highly mobile top predators? Part II: The eastern North-Atlantic. *Deep-Sea Research II* 141: 133-154. doi: 10.1016/j.dsr2.2016.06.011.

Laran, S, Authier, M, Blanck, A, Doremus, G, Falchetto, H, Monestiez, P, Pettex, E, Stephan, E, Van Canneyt, O, & Ridoux, V (2017). Seasonal distribution and abundance of cetaceans within French waters: Part II: the Bay of Biscay and the English Channel. *Deep-Sea Research II* 141: 31-40. doi: 10.1016/j.dsr2.2016.12.012

Marra, G & Wood, SN (2011). Practical variable selection for generalized additive models. *Computational Statistics and Data Analysis* 55: 2372-2387.

Pante, E & Simon-Bouhet, B (2013). marmap: a package for importing, plotting and analyzing bathymetric and topographic data in R. *PLoS ONE* 8(9): e73051. doi: 10.1371/journal.pone.0073051

Paxton, C.G.M., Burt, M.L., Hedley, S.L., Víkingsson, G.A., Gunnlaugsson, Th. and Desportes, G. (2009). Density surface fitting to estimate the abundance of humpback whales based on the NASS-95 and NASS-2001 aerial and shipboard surveys. *NAMMCO Scientific Publications* 7: 143-159.

Pike, D.G., Gunnlaugsson, T., Mikkelsen, B., Halldórsson, S.D. & Víkingsson, G.A. (2019). Estimates of the Abundance of Cetaceans in the Central North Atlantic Based on the NASS Icelandic and Faroese Shipboard Surveys Conducted in 2015. *NAMMCO Scientific Publications* 11. doi: 10.7557/3.4941

R Core Team (2020). R: A language and environment for statistical computing. R Foundation for Statistical Computing, Vienna, Austria. <https://www.R-project.org/>.

Reid, J.B., Evans, P.G.H. and Northridge, S.P. (2003). Atlas of cetacean distribution in north-west European waters. JNCC, Peterborough, UK.

Rogan, E, Cañadas, A, Macleod, K, Santos, MB, Mikkelsen, B, Uriarte, A, Van Canneyt, O, Vázquez, JA & Hammond, PS (2017). Distribution, abundance and habitat use of deep diving cetaceans in the North East Atlantic. *Deep Sea Research II: Topical Studies in Oceanography* 141: 8-19. doi: 10.1016/j.dsr2.2017.03.015

Rogan, E, Breen, P, Mackey, M, Cañadas, A, Scheidat, M, Geelhoed, S & Jessopp, M (2018). Aerial surveys of cetaceans and seabirds in Irish waters: Occurrence, distribution and abundance in 2015-2017. Department of Communications, Climate Action & Environment and National Parks and Wildlife Service (NPWS), Department of Culture, Heritage and the Gaeltacht, Dublin, Ireland. 297pp. https://secure.dccae.gov.ie/downloads/SDCU_DOWNLOAD/ObSERVE_Aerial_Report.pdf

SCANS (1995). Distribution and abundance of the harbour porpoise and other small cetaceans in the North Sea and adjacent waters. Final report under LIFE Nature project LIFE 92-2/UK/027.

SCANS-II (2008). Small Cetaceans in the European Atlantic and North Sea (SCANS-II). Final Report. University of St Andrews, UK. <http://biology.st-andrews.ac.uk/scans2/>.

Scott-Hayward, LAS, Mackenzie, ML, Donovan, Walker, CG & Ashe, E (2014). Complex Region Spatial Smoother (CReSS). *Journal of Computational and Graphical Statistics* 23:2, 340-360. doi: 10.1080/10618600.2012.762920

Víkingsson, GA, Pike, DG, Valdimarsson, H, Schleimer, A, Øien, N, Gunnlaugsson, Þ, Elvarsson, BP, Mikkelsen, B, Desportes, G, Bogason, V & Hammond, PS (2015). Effects of recent environmental changes on the distribution, abundance and feeding ecology of cetaceans in Icelandic waters. *Frontiers in Ecology and Evolution* 3: article 6. doi: 10.3389/fevo.2015.00006

Wood, SN, Bravington, MV & Hedley, SL (2008). Soap film smoothing. *Journal of the Royal Statistical Society Series B (Statistical Methodology)* 70: 931-955.

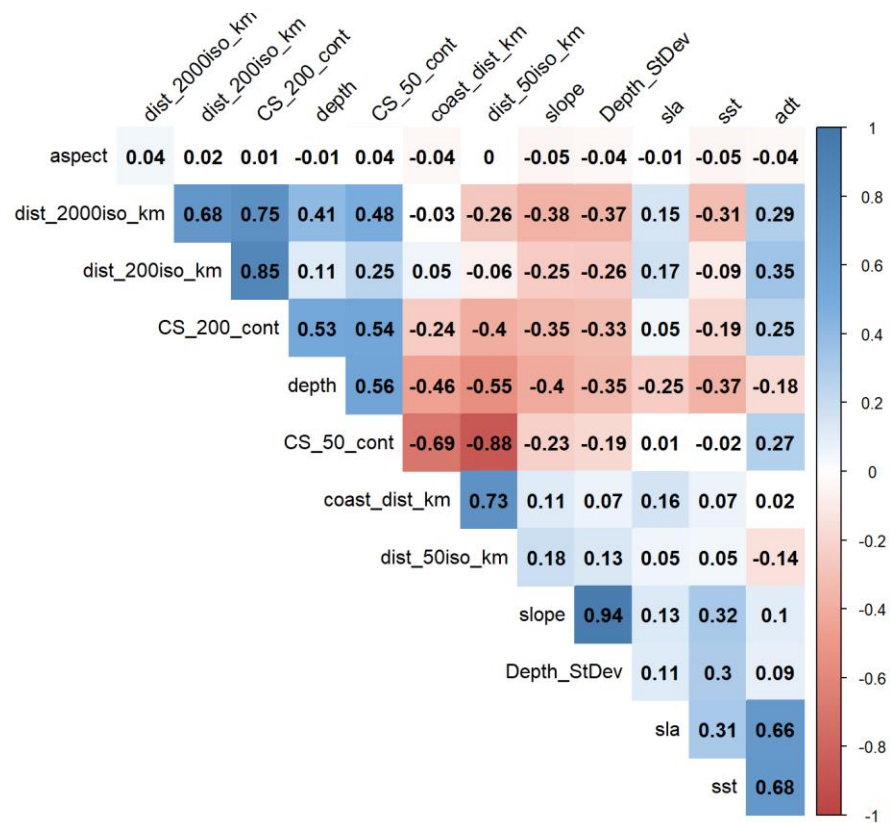
Wood, S.N. (2017). *Generalized additive models - an introduction with R*. Chapman and Hall/CRC, 496pp.

Modelled density surfaces of cetaceans in European Atlantic waters in summer 2016 from the SCANS-III aerial and shipboard surveys

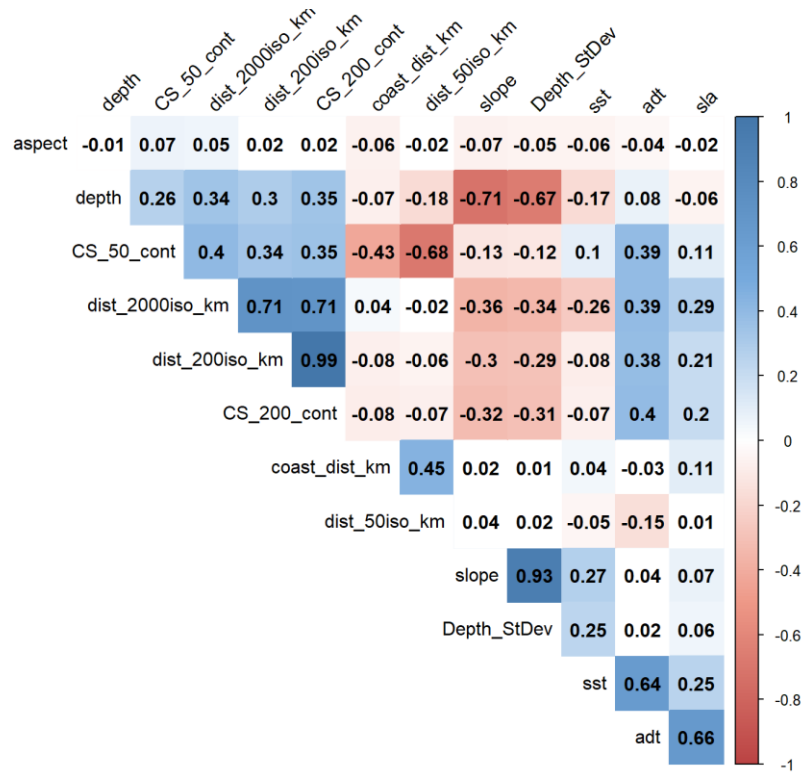
Appendices

A.1 Matrices of Pearson’s correlation coefficients between covariates for the modelled datasets. Covariates are described in Table 1. The greater the correlation (positive = blue; negative = red), the darker the colour shade in the cell.

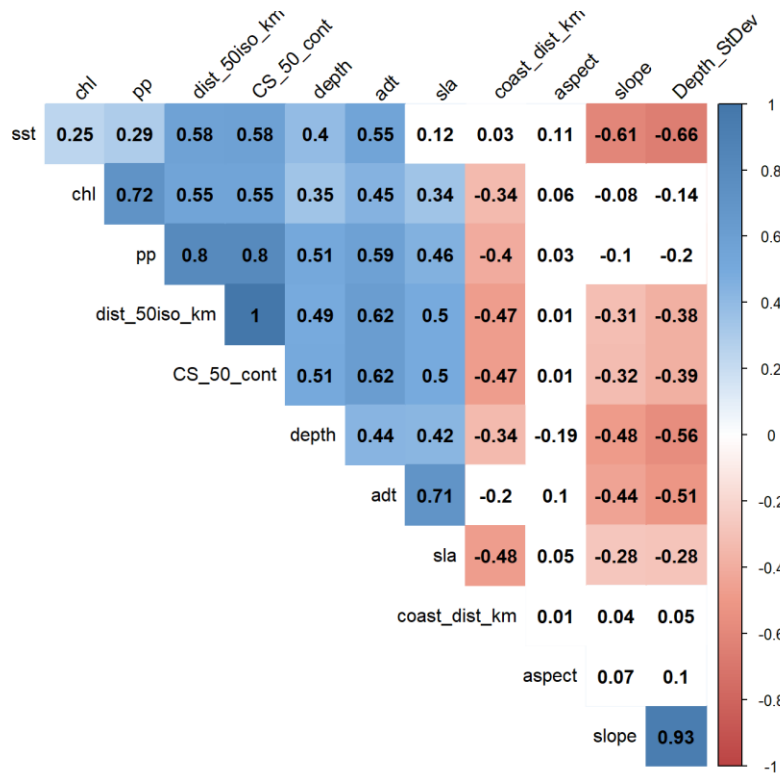
(a) SCANS-III (2016): Beaufort 0-4 (for all species except harbour porpoise)



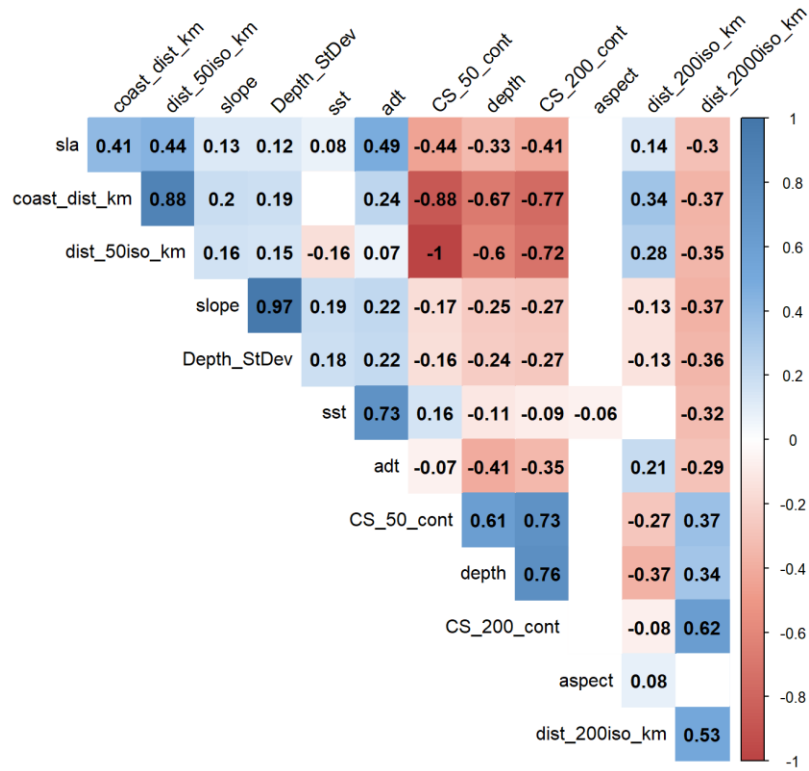
(b) SCANS-III (2016): Beaufort 0-2 (for harbour porpoise) in all blocks except Block 2



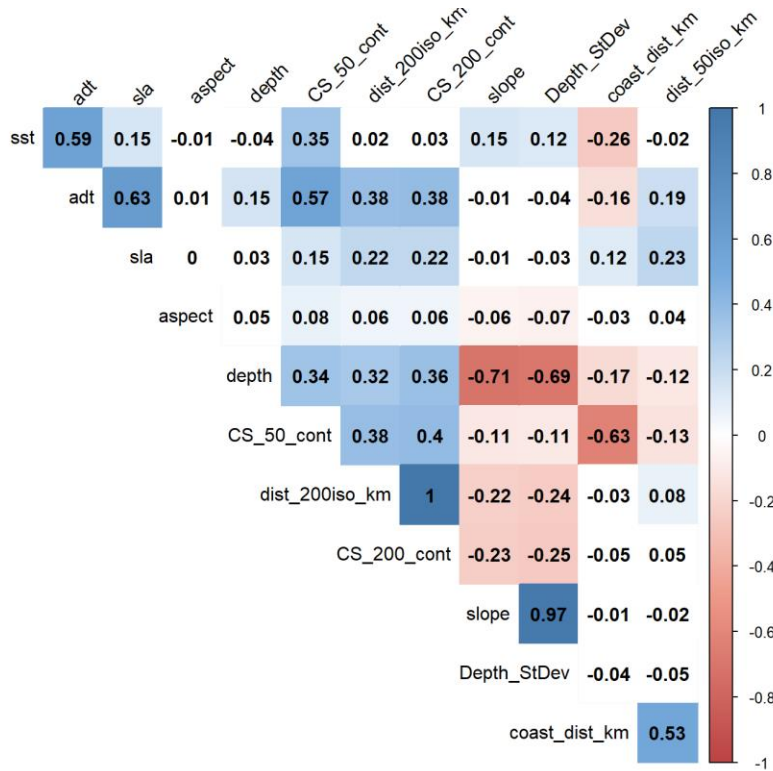
(c) SCANS-III (2016): Beaufort 0-2 (for harbour porpoise) in Block 2



(d) SCANS-II + CODA (2005/07): Beaufort 0-4 (for all species except harbour porpoise)

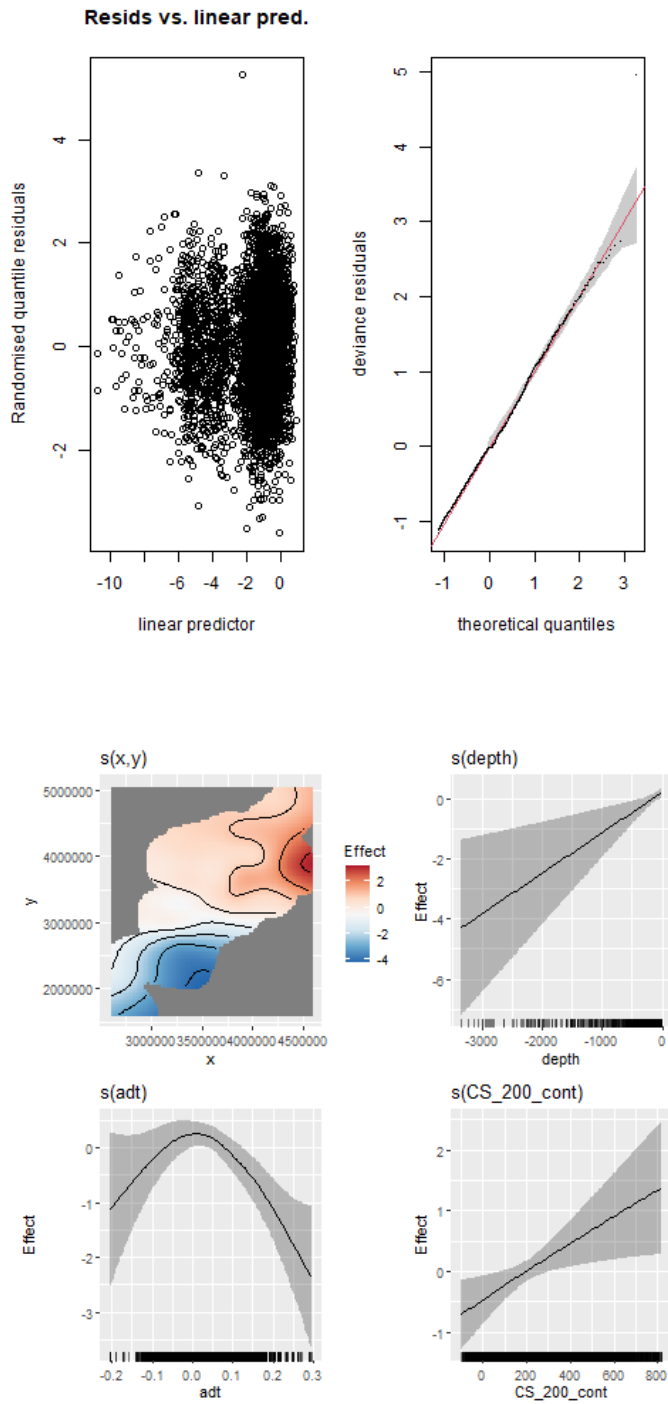


(e) SCANS-II + CODA (2005/07): Beaufort 0-2 (for harbour porpoise)

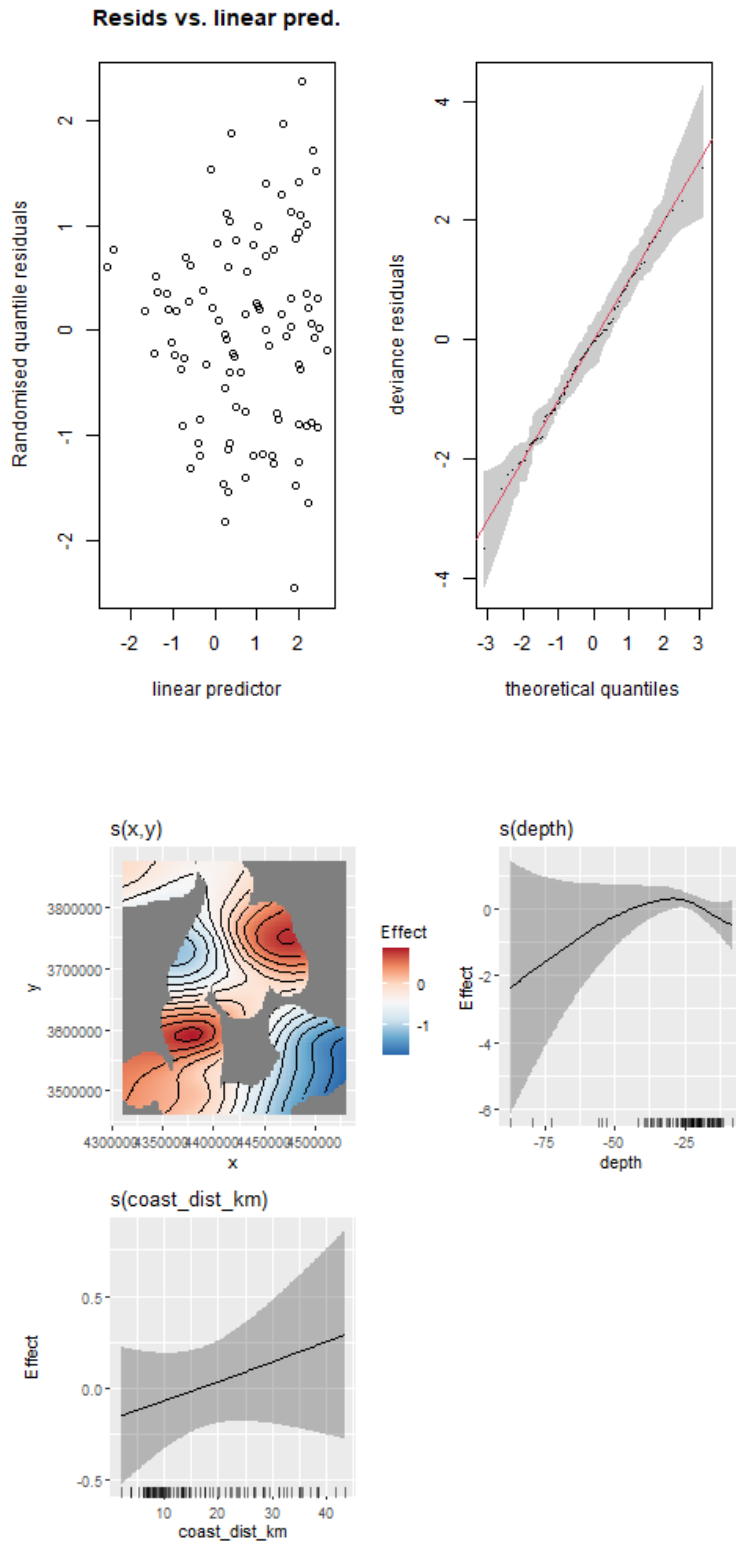


A.2 Diagnostics for final models for each species in SCANS-III (2016). For each species are shown: the randomised quantile residuals plotted against the linear predictor, the QQ plot of deviance residuals plotted against theoretical quantiles, and the fitted smooth relationships between relative density and each covariate retained in the model. Covariates are described in Table 1.

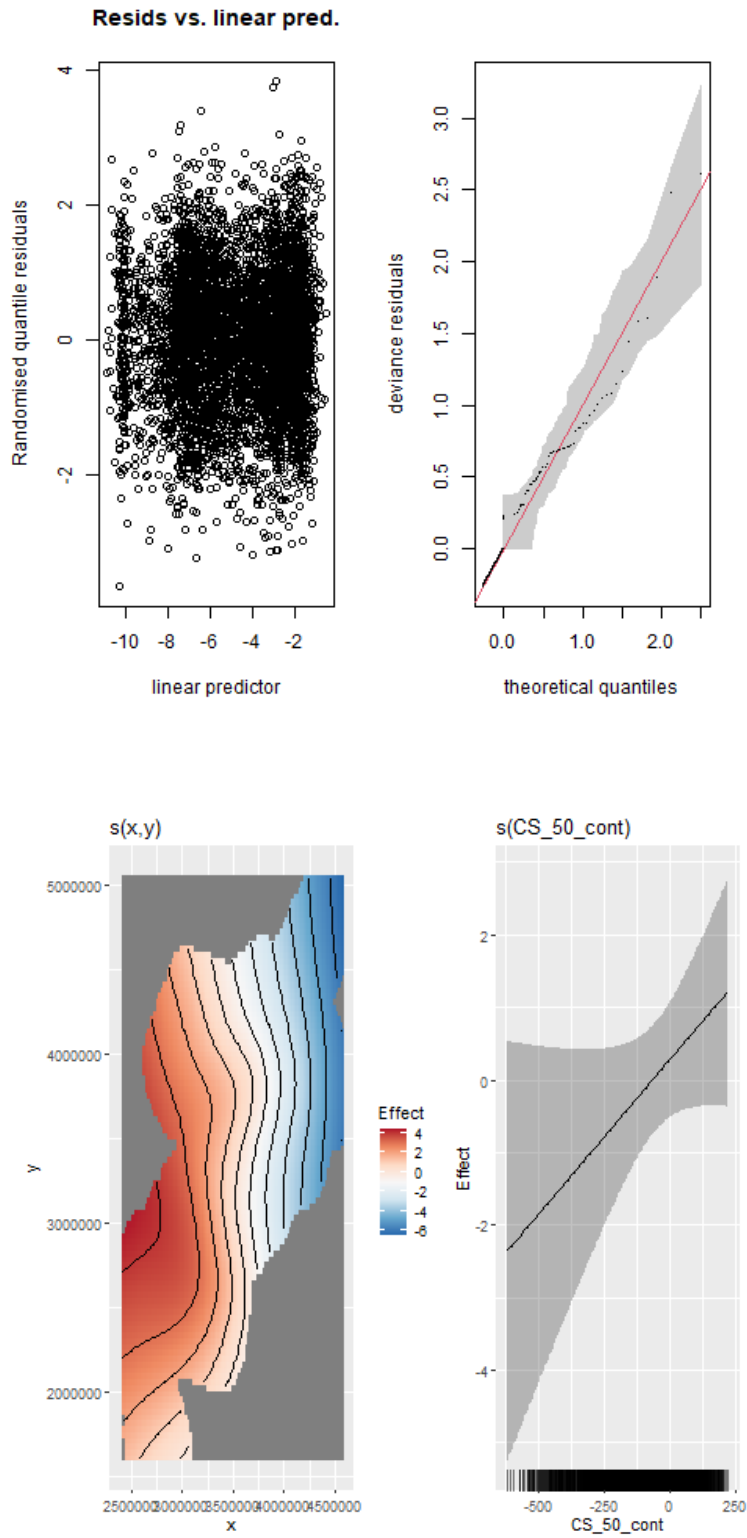
(a) Harbour porpoise individuals (excluding Block 2) – see Table 4.



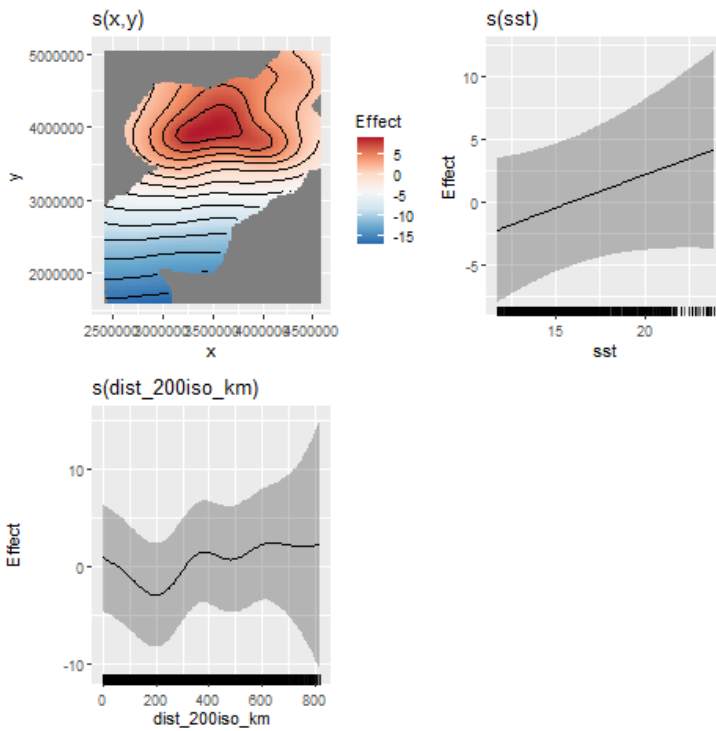
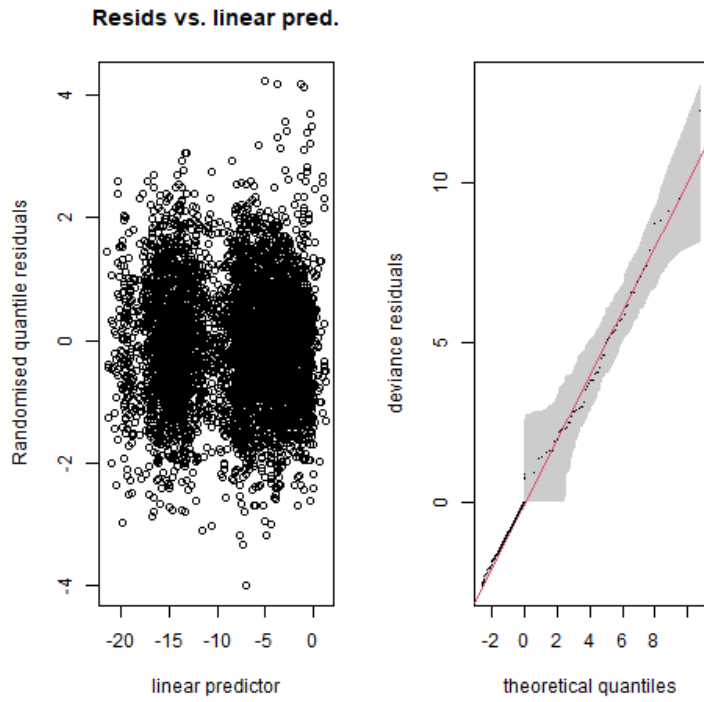
(b) Harbour porpoise individuals (Block 2 only) – see Table 4.



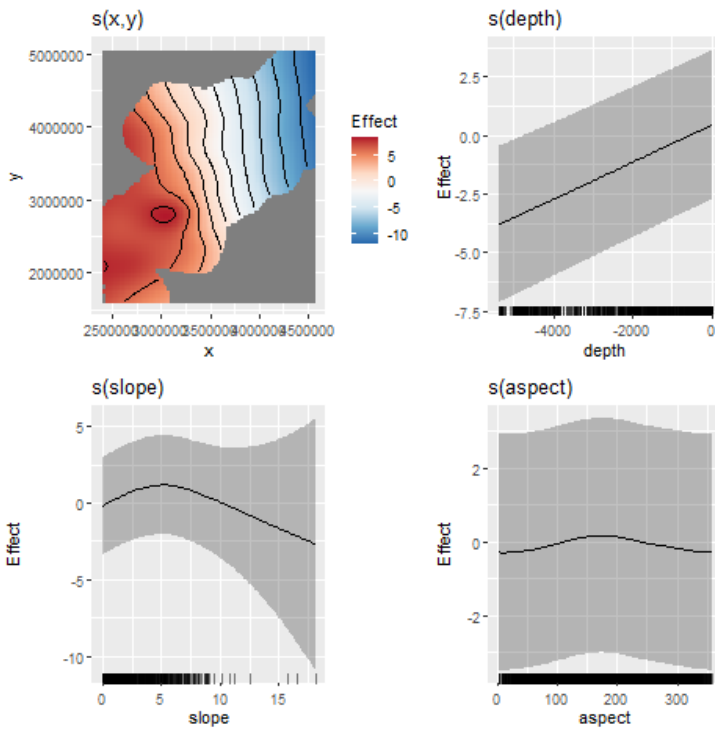
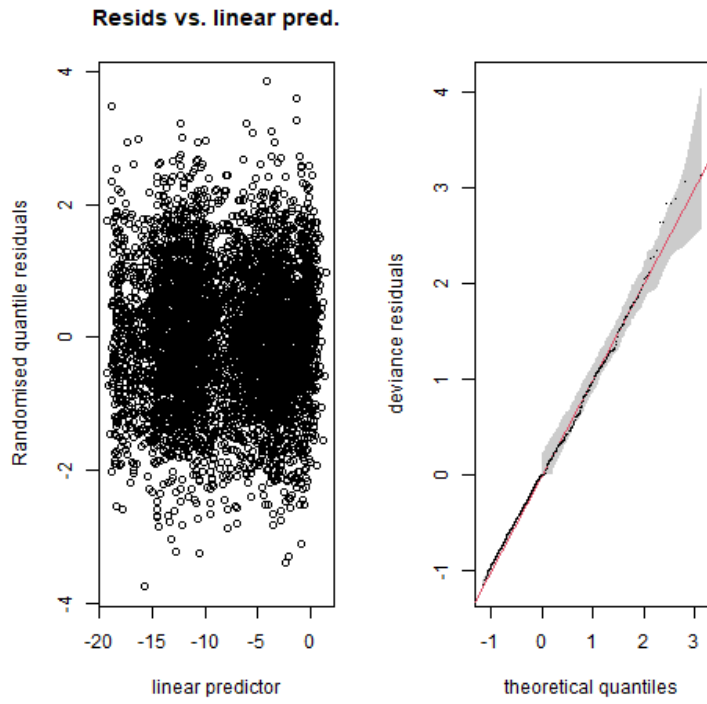
(c) Bottlenose dolphin individuals – see Table 5.



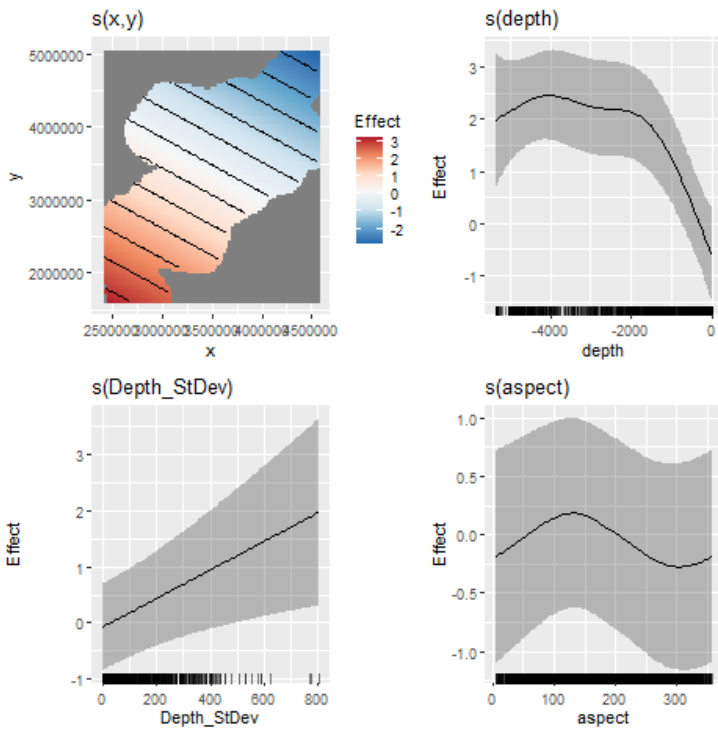
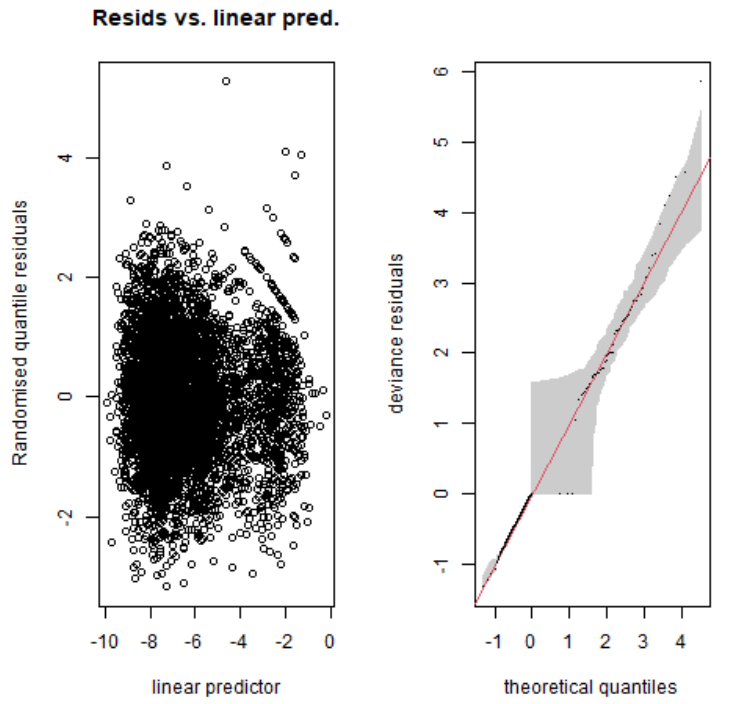
(d) White-beaked dolphin individuals – see Table 6.



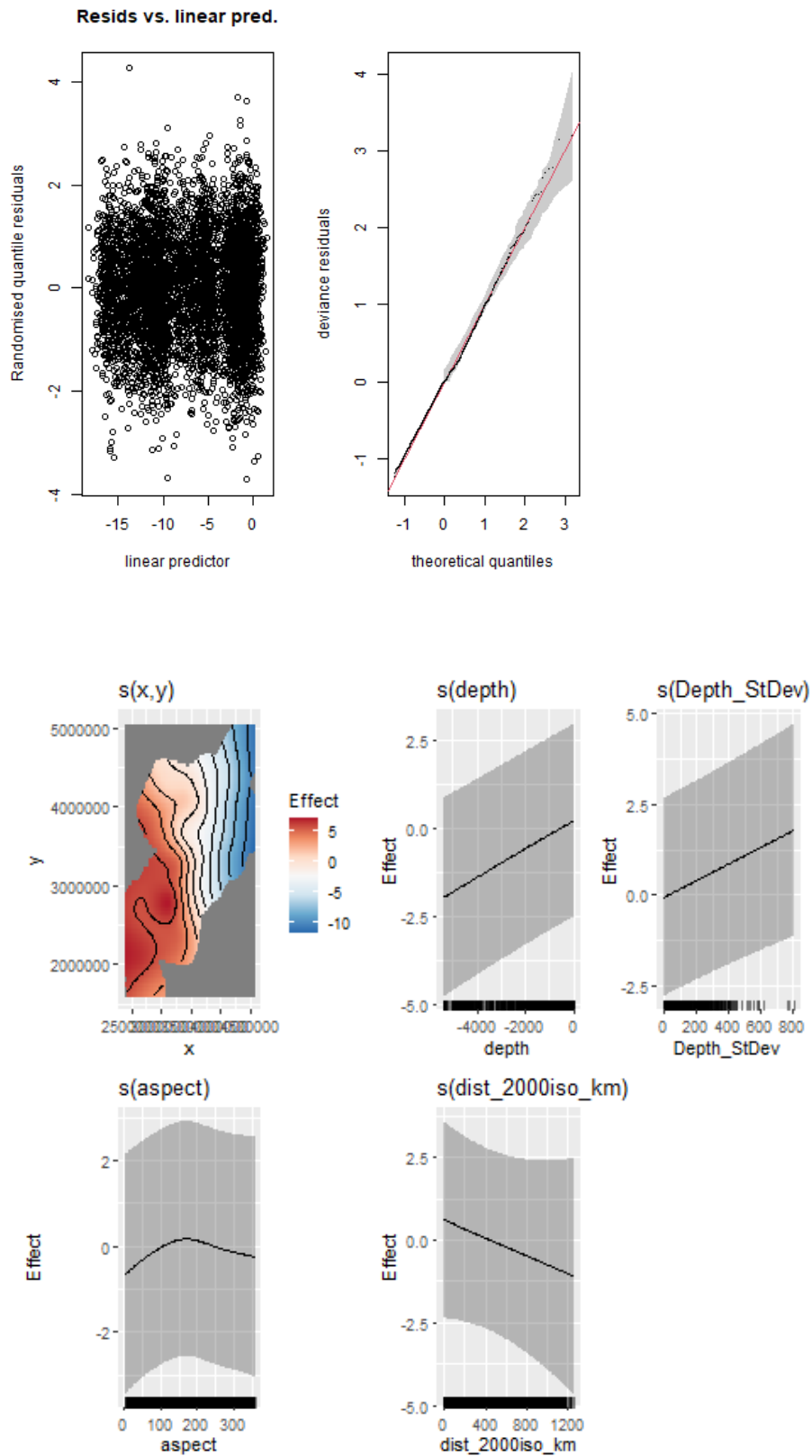
(e) Common dolphin groups – see Table 7.



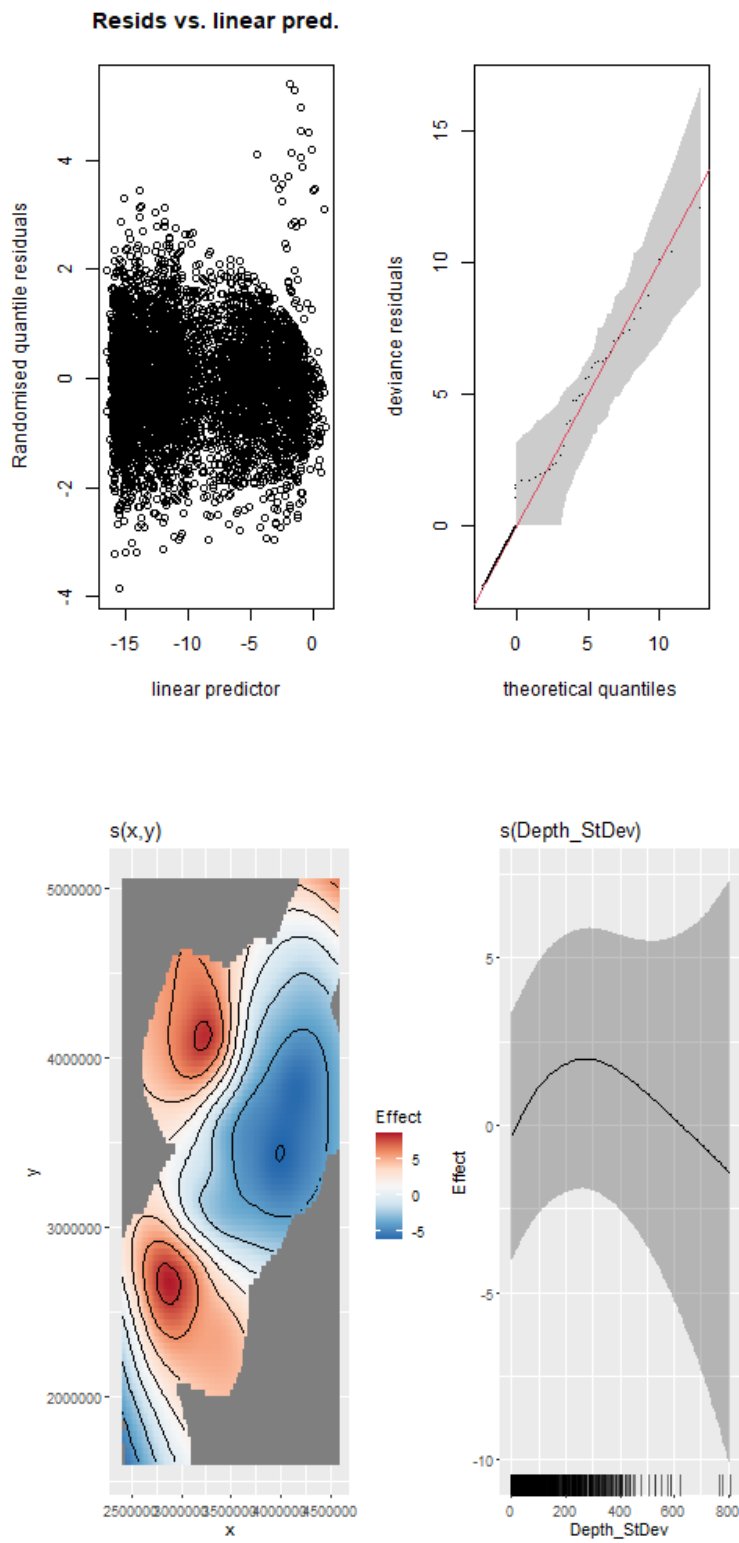
(f) Striped dolphin groups – see Table 8.



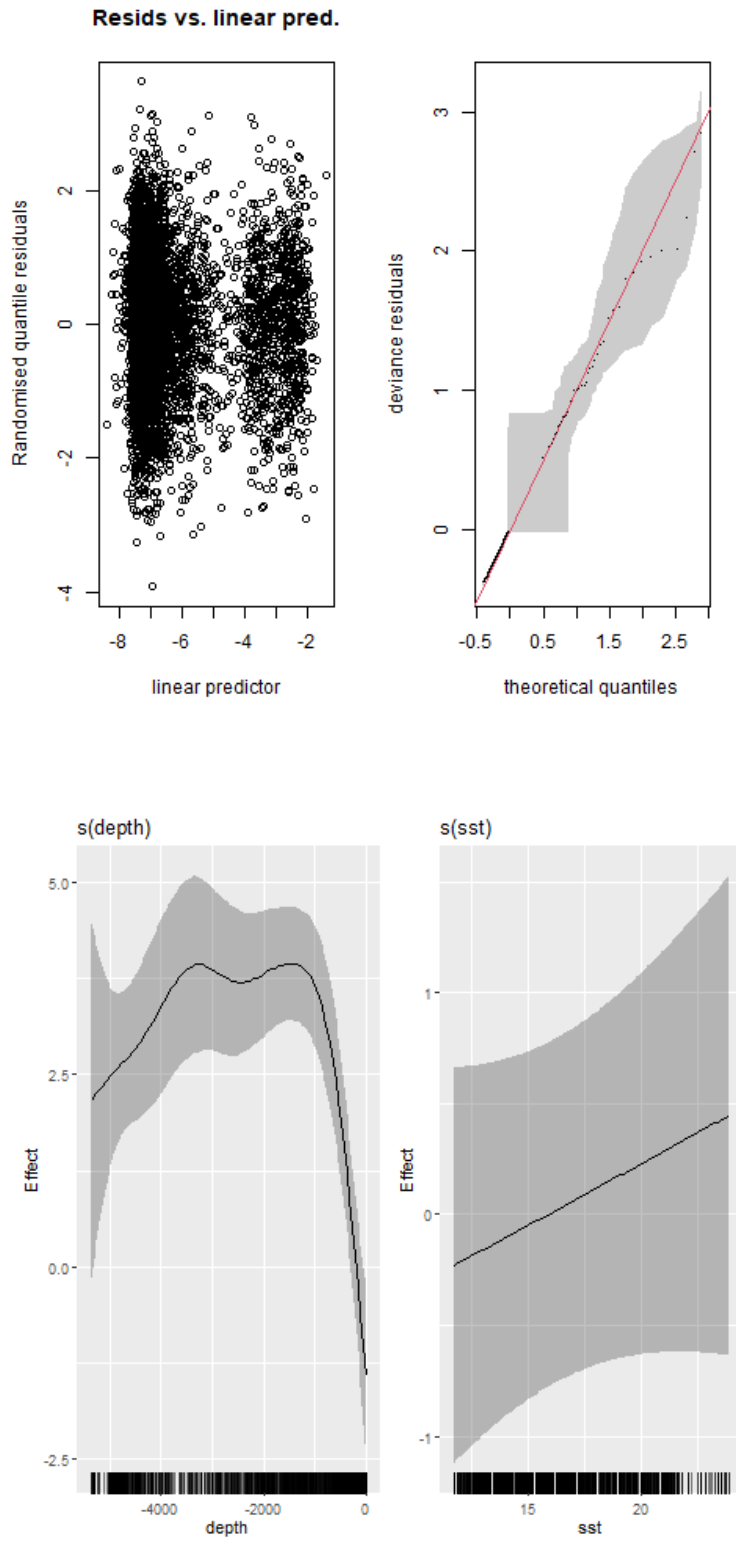
(g) Common and striped dolphin groups, including unid. common or striped dolphins – see Table 9.



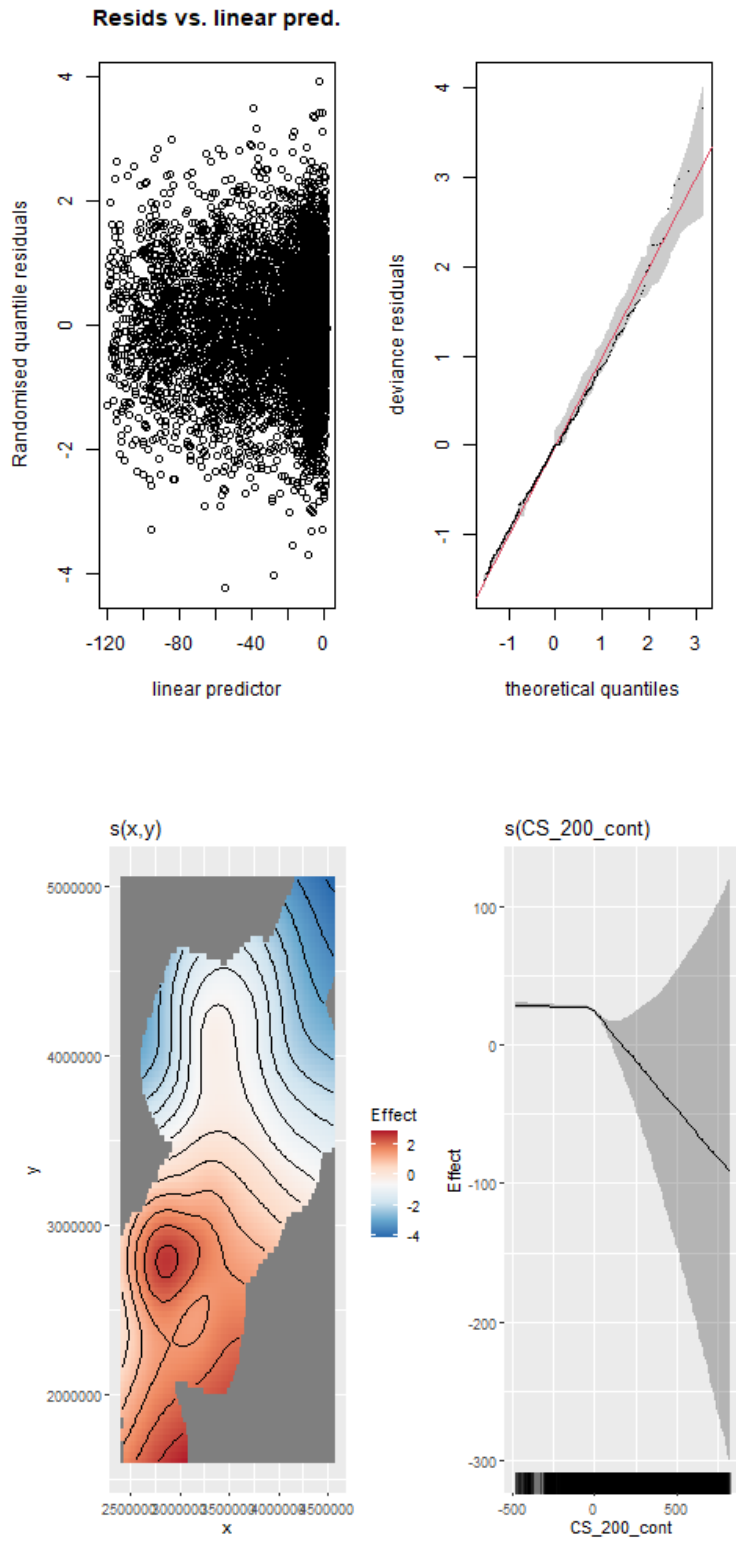
(h) Pilot whale individuals – see Table 10.



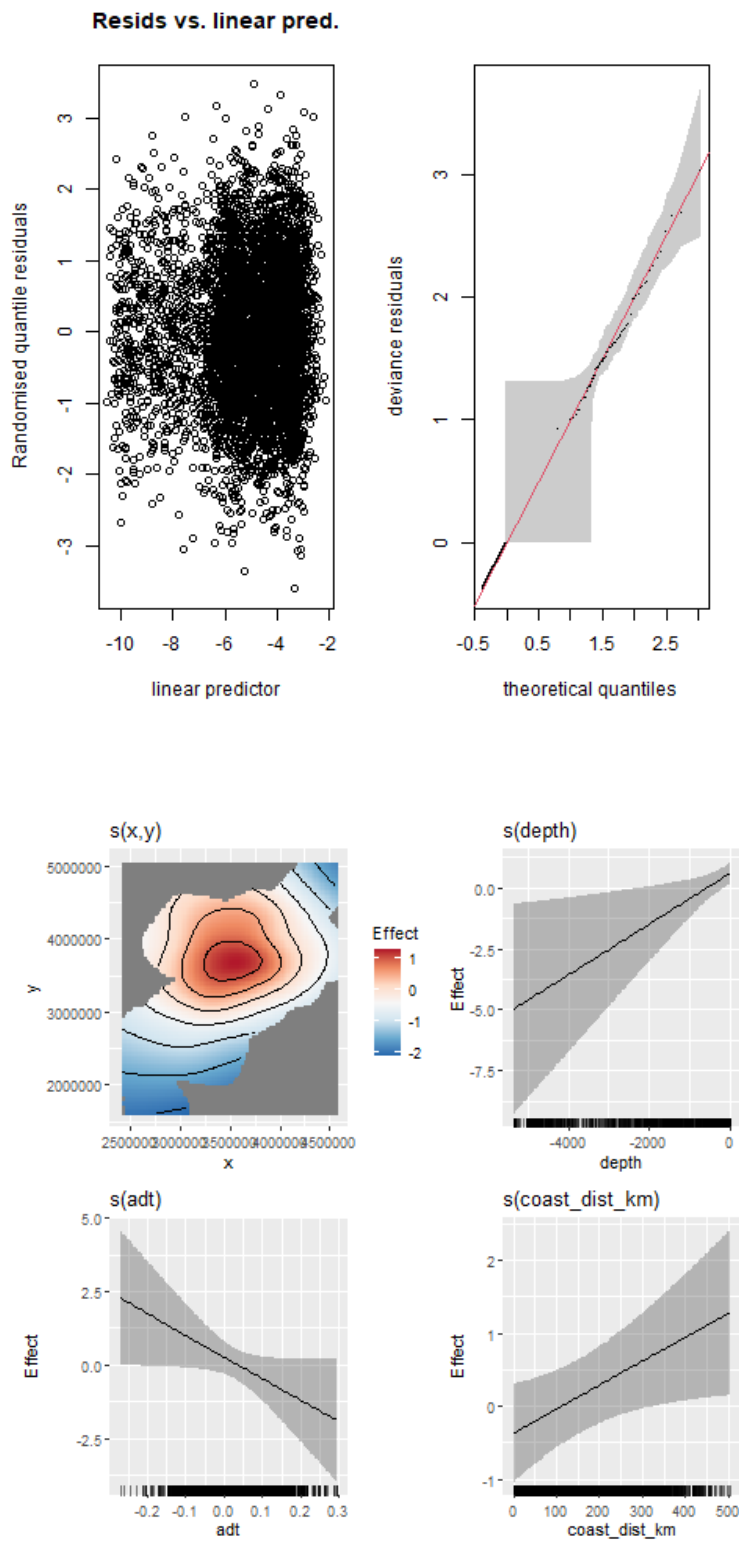
(i) Beaked whales (all species combined) individuals – see Table 11.



(j) Fin whale individuals – see Table 12.

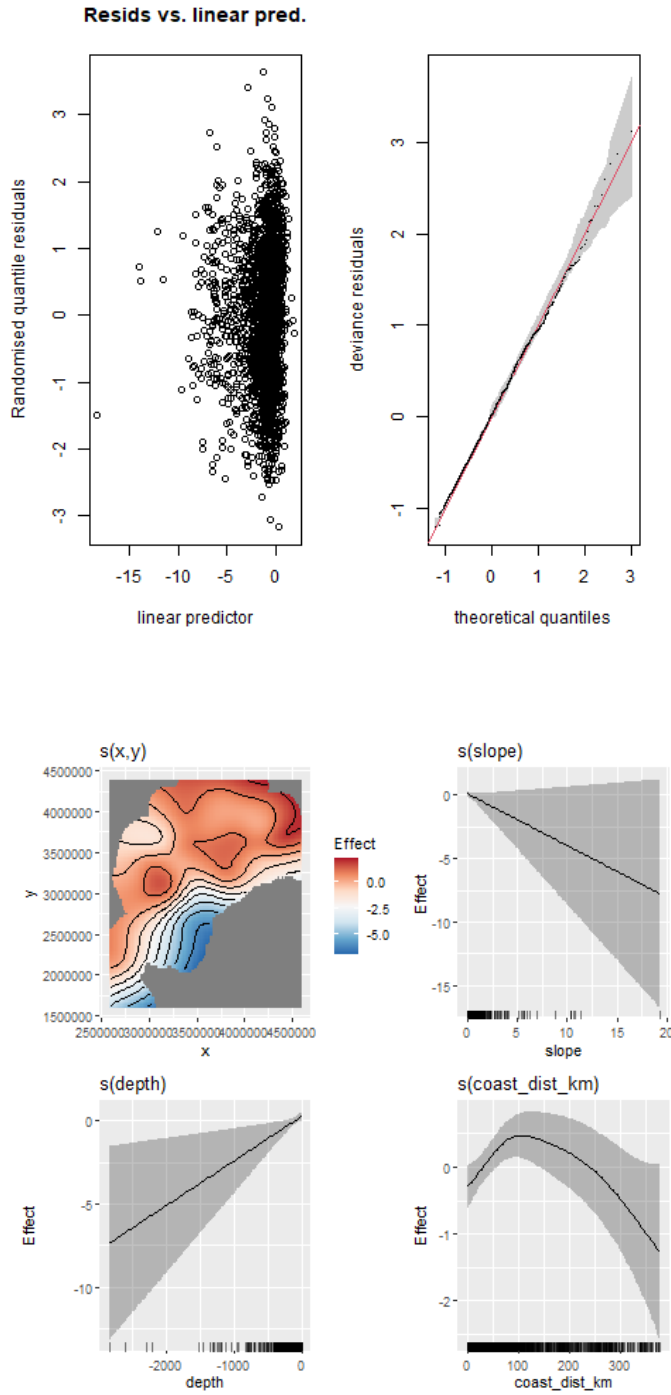


(k) Minke whale individuals – see Table 13.

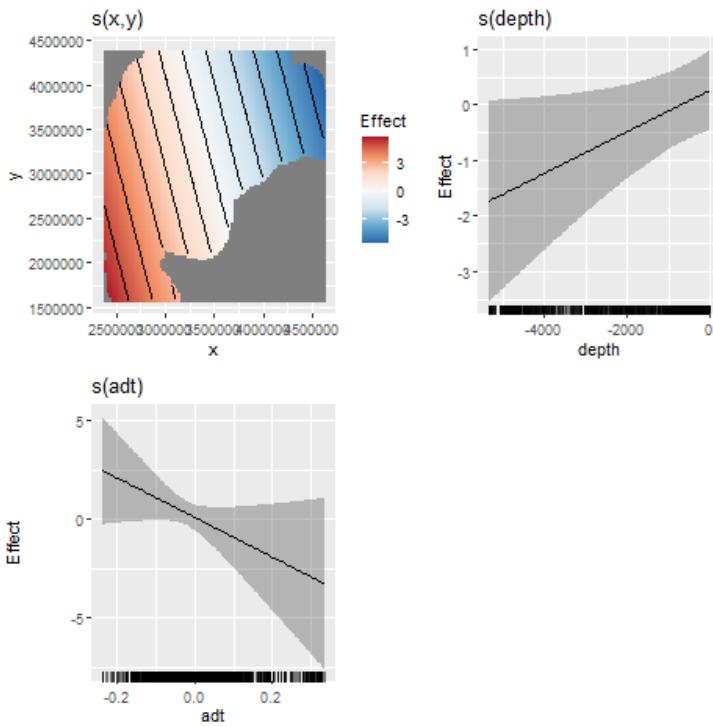
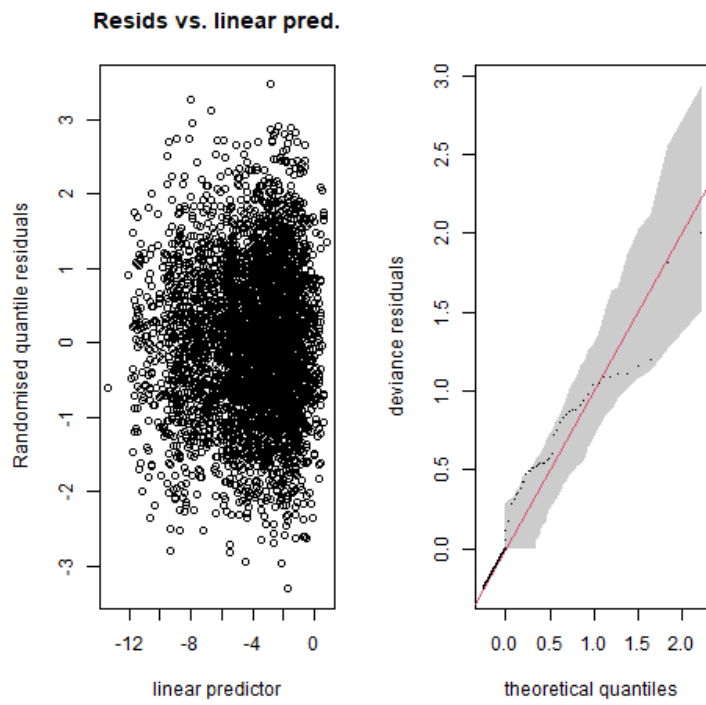


A.3 Diagnostics for selected models for each species in SCANS-II and CODA (2005/07). For each species are shown: the randomised quantile residuals plotted against the linear predictor, the QQ plot of deviance residuals plotted against theoretical quantiles, and the fitted smooth relationships between relative density and each covariate retained in the model. Covariates are described in Table 1.

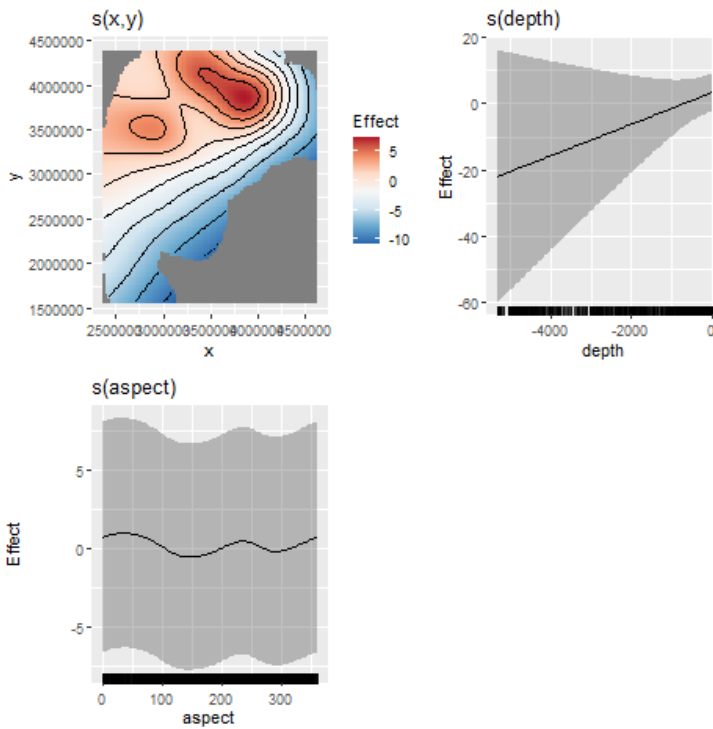
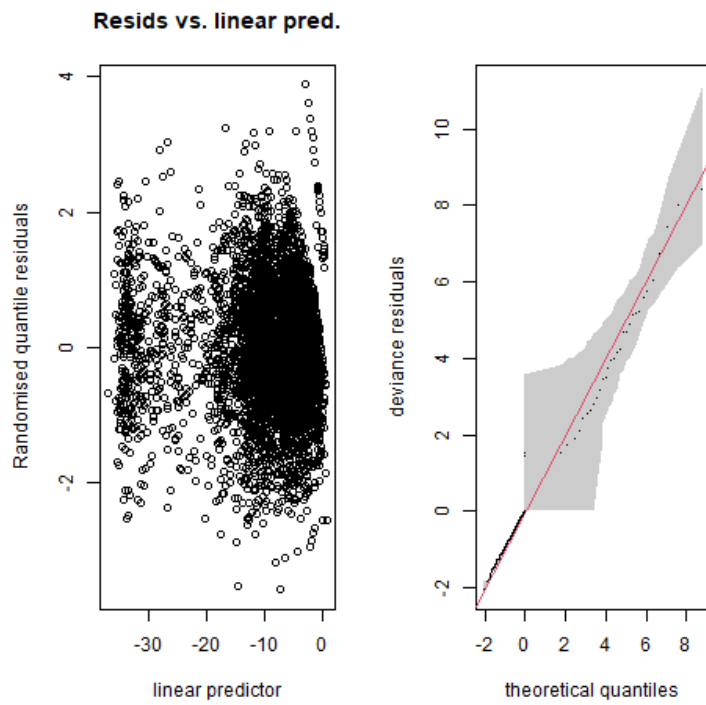
(a) Harbour porpoise individuals (SCANS-II 2005 only) – see Table 4.



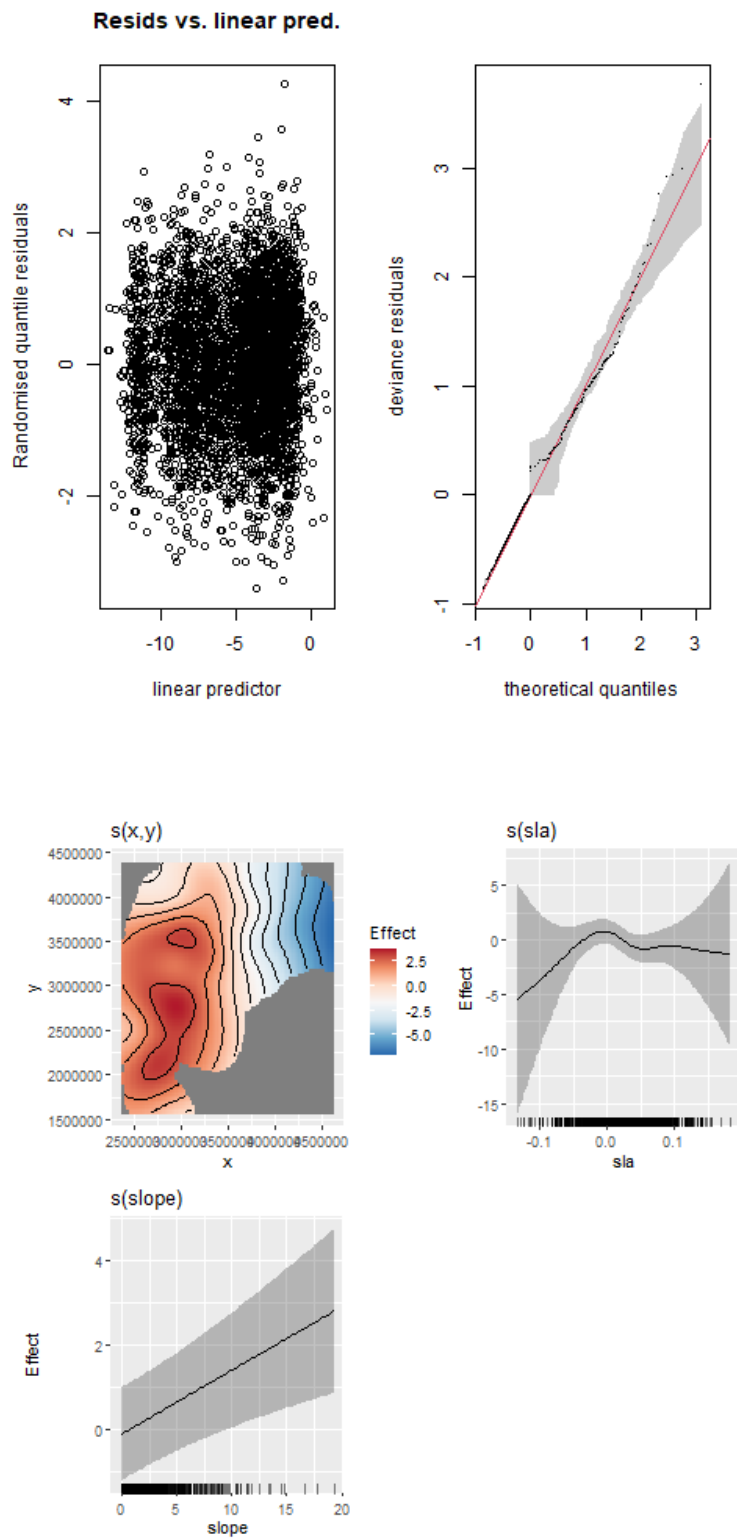
(b) Bottlenose dolphin individuals – see Table 5.



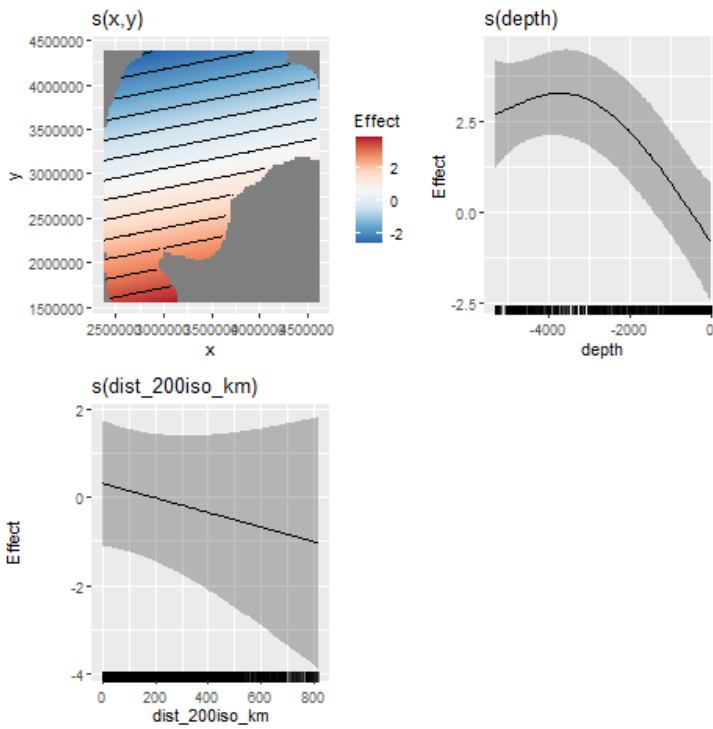
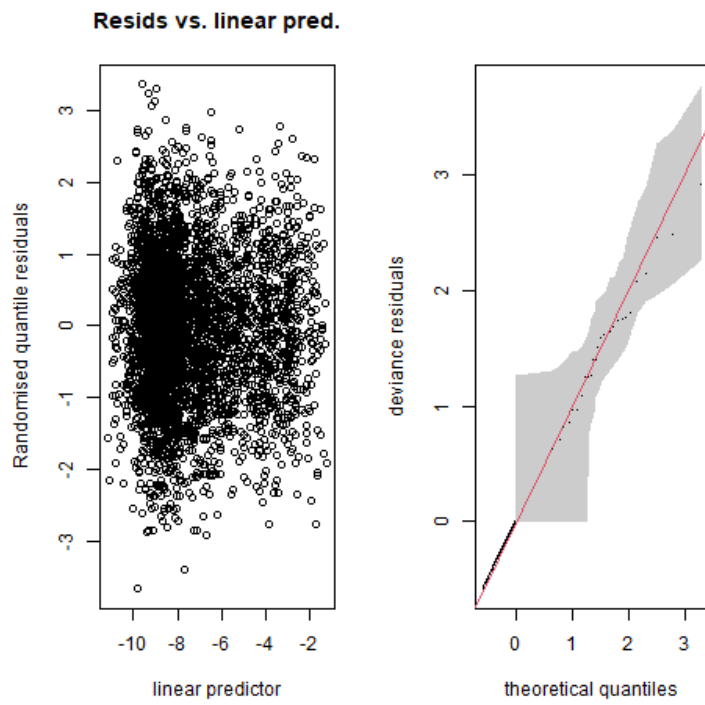
(c) White-beaked dolphin individuals – see Table 6.



(d) Common dolphin groups – see Table 7.

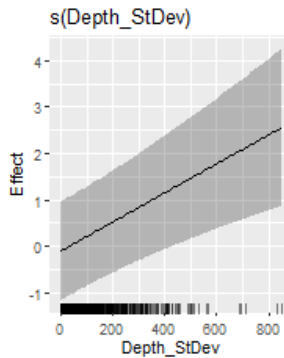
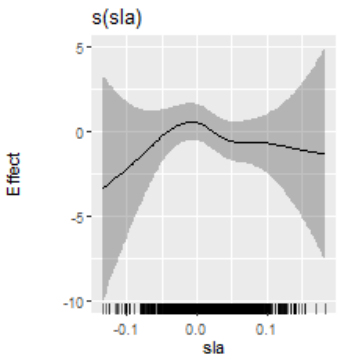
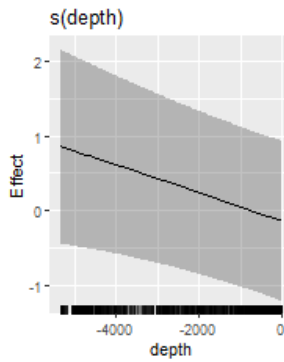
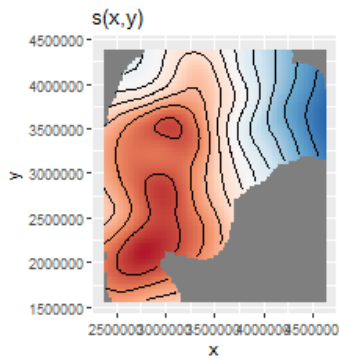
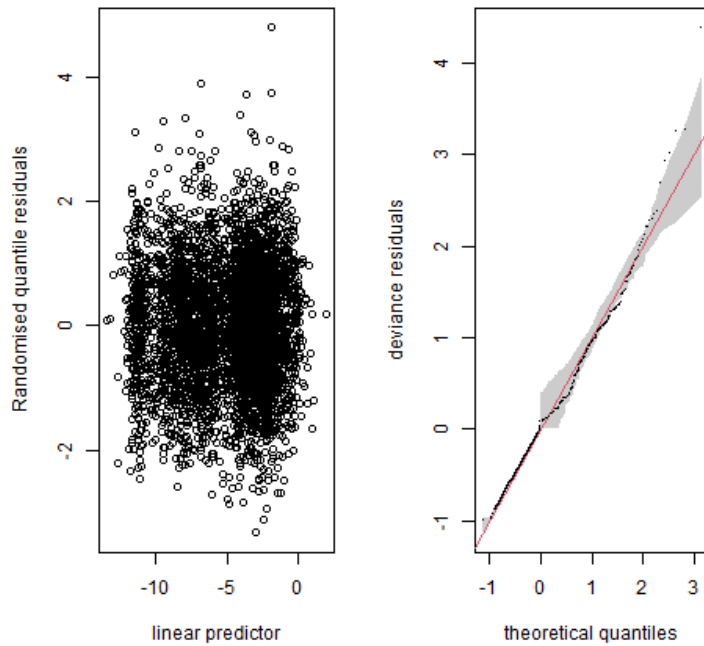


(e) Striped dolphin groups – see Table 8.

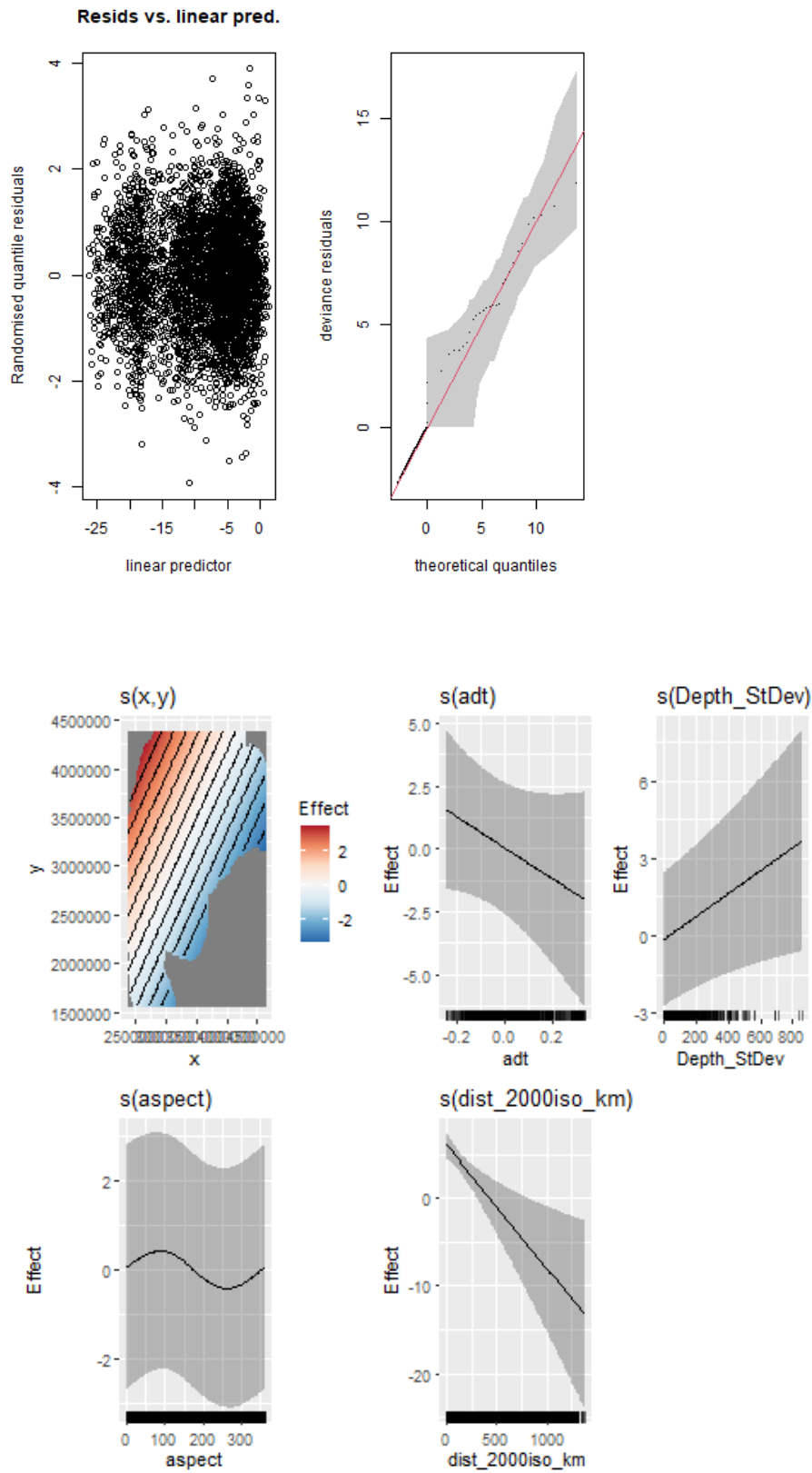


(f) Common and striped dolphin groups, including unid. common or striped dolphins – see Table 9.

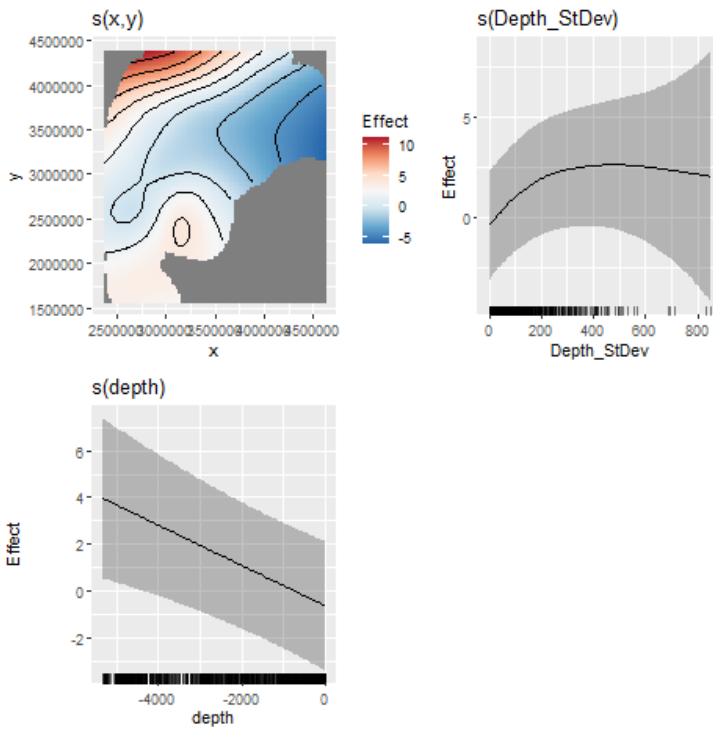
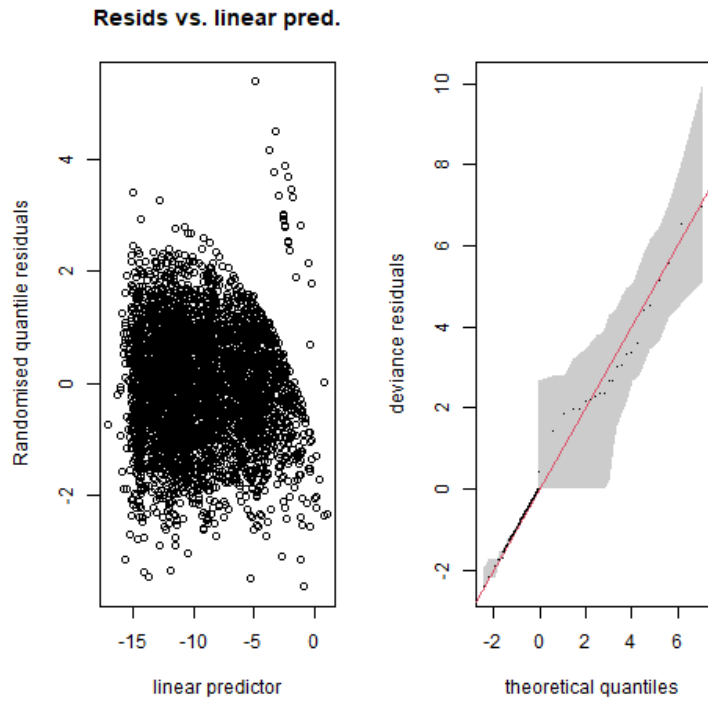
Resids vs. linear pred.



(g) Pilot whale individuals – see Table 10.

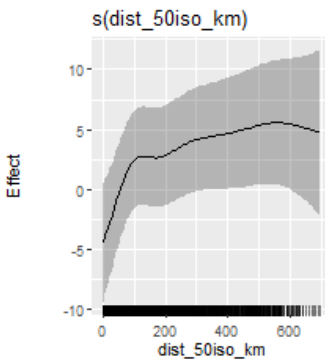
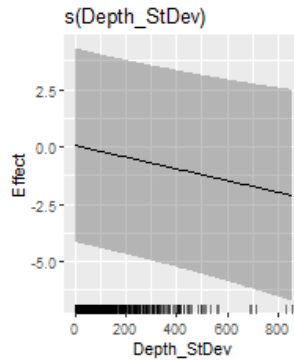
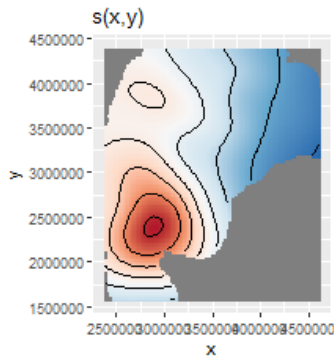
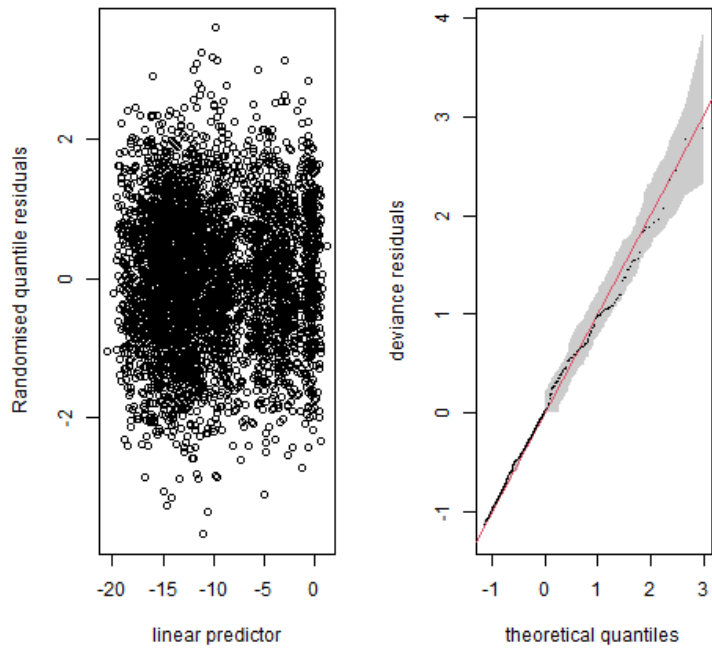


(h) Beaked whales (all species combined) individuals – see Table 11.



(i) Fin whale individuals – see Table 12.

Resids vs. linear pred.



(j) Minke whale individuals – see Table 13.

Resids vs. linear pred.

